

## **DISCLAIMER**

**This report was prepared as an account of work sponsored by an agency of the United States Government. Neither the United States Government nor any agency thereof, nor any of their employees, makes any warranty, express or implied, or assumes any legal liability or responsibility for the accuracy, completeness, or usefulness of any information, apparatus, product, or process disclosed, or represents that its use would not infringe privately owned rights. Reference herein to any specific commercial product, process, or service by trade name, trademark, manufacturer, or otherwise does not necessarily constitute or imply its endorsement, recommendation, or favoring by the United States Government or any agency thereof. The views and opinions of authors expressed herein do not necessarily state or reflect those of the United States Government or any agency thereof. Reference herein to any social initiative (including but not limited to Diversity, Equity, and Inclusion (DEI); Community Benefits Plans (CBP); Justice 40; etc.) is made by the Author independent of any current requirement by the United States Government and does not constitute or imply endorsement, recommendation, or support by the United States Government or any agency thereof.**

**SANDIA REPORT**

SAND2025-00019

General Proprietary Business Information – Basic

Printed February 2025

**Sandia  
National  
Laboratories****SNL NSTTF Heliostat Refurbishment Project Final Report**

Kenneth M. Armijo, Ansel Blumenthal, Luis Garcia-Maldonado and Lonnie Haden

Controlled by: Sandia National Laboratories, Kenneth M. Armijo

Prepared by  
Sandia National Laboratories  
Albuquerque, New Mexico  
87185 and Livermore,  
California 94550

Issued by Sandia National Laboratories, operated for the United States Department of Energy by National Technology & Engineering Solutions of Sandia, LLC.

**NOTICE:** This report was prepared as an account of work sponsored by an agency of the United States Government. Neither the United States Government, nor any agency thereof, nor any of their employees, nor any of their contractors, subcontractors, or their employees, make any warranty, express or implied, or assume any legal liability or responsibility for the accuracy, completeness, or usefulness of any information, apparatus, product, or process disclosed, or represent that its use would not infringe privately owned rights. Reference herein to any specific commercial product, process, or service by trade name, trademark, manufacturer, or otherwise, does not necessarily constitute or imply its endorsement, recommendation, or favoring by the United States Government, any agency thereof, or any of their contractors or subcontractors. The views and opinions expressed herein do not necessarily state or reflect those of the United States Government, any agency thereof, or any of their contractors.

Printed in the United States of America. This report has been reproduced directly from the best available copy.



## ABSTRACT

This document provides an overview of technical efforts at Sandia National Laboratories (SNL), National Solar Thermal Test Facility (NSTTF), for the U.S. Department of Energy (DOE), Solar Energy Technologies Office (SETO), SNL Heliostat Refurbishment project. Sandia continues to pursue innovative concentrating solar power (CSP) and thermal (CST) research in order to enhance commercial performance and reduce LCOE and LCOH of concentrating solar energy. In the course of this history, Sandia has developed many tools and capabilities for analysis and improvement of heliostats, including design, construction, measurement, validation and utilization of large-scale testing facilities for the full characterization of heliostats. The heliostat field can generate a peak flux of up to  $350 \text{ W/cm}^2$  and  $6 \text{ MW}_{\text{th}}$  total power which has allowed state-of-the-art research and development (R&D) for a variety of projects spanning five decades. The heliostat field has foundations, power, and communications available for testing of innovative custom heliostats utilizing the National Solar Thermal Test Facility (NSTTF) world-class heliostat evaluation and metrology laboratory. These include a custom controls system, beam characterization system (BCS), heliostat canting and alignment, long-range beam analysis, wind modal analysis, and tracking /and pointing analysis. The heliostat field, comprised of 218 heliostats has endured over four decades of operation where some components have reached the end of life, or have experienced reliability issues and wear. This project was facilitated to address key areas of the NSTTF heliostat field that require upgrades or refurbishment to ensure confident operational utilization of the heliostat field for DOE and non-DOE projects (e.g., DOD, NASA, US Missile Def. Agency, etc.). Private companies, including many small businesses and start-ups, have been working to commercialize CSP systems where critical advanced controls and wireless systems require more substantive evaluation prior to commercial deployment. This work has upgraded the controls hardware and software to allow for improved functionality and control, flexibility for assessing varying commercial heliostat configurations, as well as integration and testing of novel R&D heliostats. Additionally, this work has enabled the field to better adapt to both closed loop controls customer systems as well as future wireless control capabilities.

This page is left blank

## **ACKNOWLEDGEMENTS**

Sandia National Laboratories is a multi-mission laboratory managed and operated by National Technology & Engineering Solutions of Sandia, LLC, a wholly owned subsidiary of Honeywell International, Inc., for the U.S. Department of Energy's National Nuclear Security Administration under contract DE-NA0003525. The team would also like to acknowledge funding and support by the U.S. Department of Energy, Solar Energy Technologies Office (SETO), a department within the Energy Efficiency and Renewable Energy (EERE) Office for sponsorship of this project.

This page is left blank

## TABLE OF CONTENTS

Abstract .....	3
Acknowledgements.....	5
Table of Contents .....	7
1. Project Background.....	9
2. Project Milestones .....	11
Milestone 1.1.1 – Heliostat Hardware Upgrades .....	11
Milestone 1.1.2 – Wireless Communications Upgrades.....	11
Milestone 1.2.1 – Protocol Development & Technical Down-Selections .....	12
Milestone 1.2.2 – Final Controls Upgrades and Communications Validation .....	12
3. Project Overview.....	14
3.1 Status and limitations of current controls system, software and hardware .....	14
4. Project Results & Discussion.....	16
4.1 Task 1.0 NSTTF Heliostat Field Hardware Upgrades.....	16
4.1.1 Fiber Optic Cabling .....	16
4.1.2 Software Development.....	17
4.1.3 cRIO Programmable Logic Controller (PLC) Upgrades.....	25
4.1.3 Heliostat Field Wireless Communications Upgrades.....	26
4.1.4 Site Integrated NAS Data Historian.....	43
4.1.5 Hardware & Software Upgrades Small-Scale Test Beds.....	44
4.1.6 All-Sky Camera Cloud Tracking Capability.....	45
4.1.7 Heliostat On-Board Power Development.....	46
4.1.8 Field Upgrades Deployment and Commissioning .....	48
5. Full Field Deployment & Commissioning.....	56
6. NSTTF Closed Loop Controls Development .....	62
7. Overall NSTTF Heliostat Refurbishment Effort Improvements .....	69
7.1 Flux Improvement by Heliostat Field BCS Scanning Techniques .....	70
7.2 Tracking Performance Improvements .....	73
7.3 Theoretical Sun Position Calculation Improvement.....	75
8. References.....	77
Distribution.....	78

This page left blank

## 1. PROJECT BACKGROUND

The original Heliostat Field Software Control dates back to the early 1980's. Back in the 1980's SNL used analog computers to send signals via BNC cables to perform motion movements at the Heliostat control box. To this day, the same power line is used to power the Heliostat Field. That consists of 480V 3 Phase at 100-amp power rating. The Heliostat Field has been the lynchpin of the entire NSTTF to operate and advance CSP research since the Oil crisis of the 1970s. The original motors and the same drive encoders have been used to perform the motion profiles required for testing, CSP research and optical metrology. Figure 1 shows the 1980's Heliostat Field in operation using analog computers.

The Heliostat Field has supported various research areas through its 45<sup>th</sup> anniversary. This included concentrated thermal research, defense work and aerospace research. With the large reflective area of approximately 132 m<sup>2</sup>, the NSTTF heliostats can facilitate well-controlled flux with well-canted individual facets up to 30 solar constants of flux into a desired target.

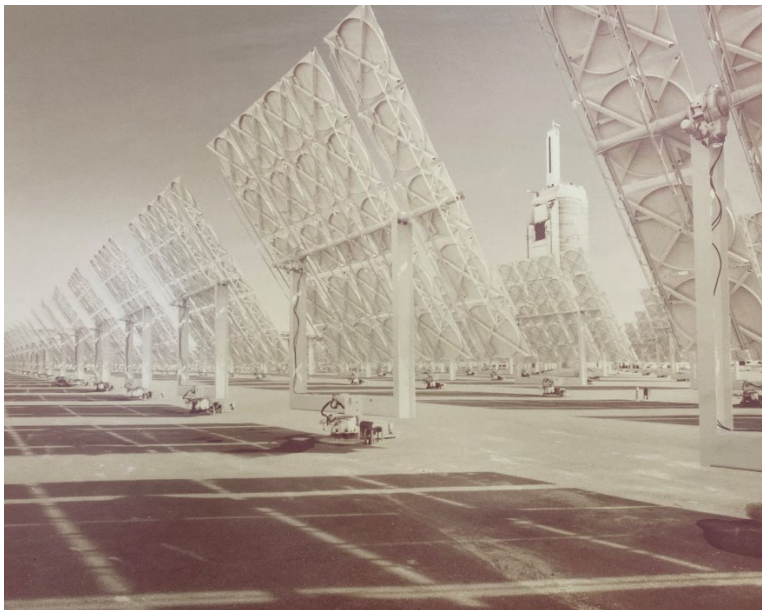


**Figure 1.** Heliostat Field been controlled using Analog Computers.

The old control software of the NSTTF Heliostat Field used a 2008 LabVIEW development library, which was supported with Windows 7 operating system only. Sandia stopped supporting Windows 7 at the end of 2019 at the same time as Microsoft. This created a major issue for the NSTTF. To maintain the operation of the Heliostat Field computer running Windows 7, the NSTTF had to submit a cyber security patch application to allow us to purchase an original copy from a 3<sup>rd</sup> party vendor because there was not a backup computer to operate the field. The security patch took over 1 year to get approved. This short-term solution gave the NSTTF enough time to discuss the potential update of the Heliostat Controllers and the Main Control Software to a newer version of LabVIEW and Windows 11 as the operating system.

Another major problem with the control software was the architecture. The architecture used was opaque and inhospitable for any non-LabVIEW programmers. It contained password protected sub systems that would allow tracking and other important functions. To decipher this architecture would have taken more time than to just build it from scratch.

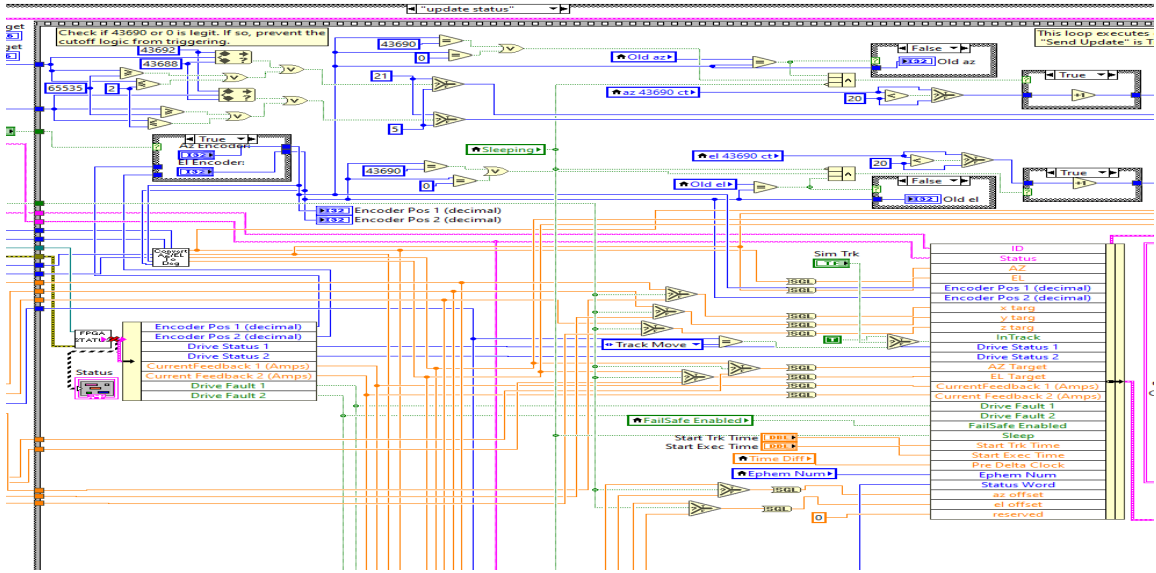


Figure 2. 2008 LabVIEW old code.

Figure 2 shows the Graphical User Interface of the Old Control Software, which contains graphical elements that date back to 2008. For this Heliostat Field Refurbishment, we kept a similar graphical Heliostat layout to allow the Heliostat Operators to keep the same flow of operations. This will allow for an easier transition from the old to the new control software.

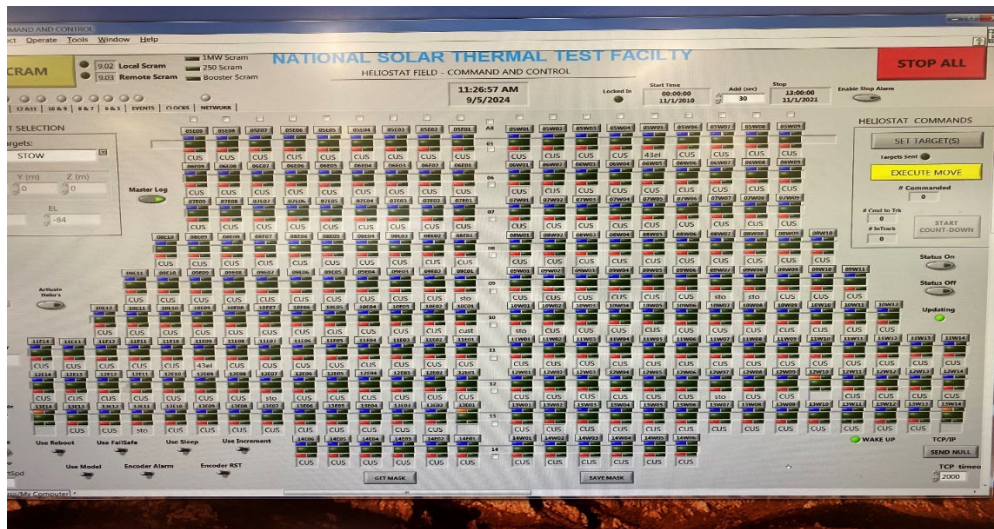


Figure 3. 2008 Heliostat Field Control Software Graphical User Interface (GUI).

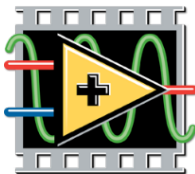


Figure 4. LabVIEW 8.6 released in 2008.

## 2. PROJECT MILESTONES

There were four milestones that were setup within the technical work plan (TWP) at the start of this investigation to measure progress throughout the project. These milestones can be seen in the Tables below. For each of these milestones a brief breakdown of how this assessment tool was used for each is described below.

### Milestone 1.1.1 – Heliostat Hardware Upgrades

For milestone 1.1.1, the team utilized the Table 1 assessment tool to track hardware upgrades, particularly for the 218 cRIOs which were replaced, that included firmware and other software upgrades that needed to be facilitated for each respective unity. The team also used this tool to baseline the hardware upgrades (which included fiber optic cabling throughout the heliostat field and wireless comms hardware) against current 3-wire network cabling and our old 2005 cRIO PLCs.

**Table 1.** Milestone 1.1.1 Assessment Tool Excerpt

Description	Metric	Success Value	Assessment Tool	Metric Justification
The team will facilitate critical communications, DAQ, PLC and DCS hardware upgrades for the NSTTF heliostat field. This will include equipment upgrades via standard signal evaluation at the NSTTF, which is necessary to establish a resilient heliostat field communications testing system. The team will also leverage previously facilitated commissioning data-driven technology-risk mitigation strategies to include maintenance programs (corrective or preventive). Signal processing confirmation will be facilitated through LabVIEW NI MAX Signal Processing & Evaluation software. The team will also facilitate electrical continuity testing with signal injection to validate reliable communication with newly installed fiber optic cabling.	<ul style="list-style-type: none"> <li>• Upgraded NI cRIO chassis and firmware upgrades</li> <li>• Completion of fiber optic cabling upgrades</li> <li>• Instances of wireless communication loss of signal (LOS) after evaluation</li> </ul>	<ul style="list-style-type: none"> <li>• 100%</li> <li>• 8 rows</li> <li>• 0%</li> </ul>	Current practice at the NSTTF is using ca. 2005 cRIO modules and three-wire communication network cabling.	Required to ensure up to date hardware installations, required to pair with the new software licenses within the heliostat field and control room.

### Milestone 1.1.2 – Wireless Communications Upgrades

For milestone 1.1.2, the team utilized the Table 2 assessment tool to track hardware development and installation of a new wireless communications system between the central DSC computer and each of the heliostat PLCs. Here, the team used the Milestone Assessment tool to track progress with the installation and performance communications checkouts with each of the PLCs. Although this mostly pertained to the Wifi system, the metric monitoring of LOS and signal errors, was also tracked for the wireless Mesh network development as part of another DOE Heliocon RFP project.

**Table 2.** Milestone 1.1.2 Assessment Tool Excerpt

Description	Metric	Success Value	Assessment Tool	Metric Justification
The team will stand up a Wifi baseline wireless controls system for the current NSTTF heliostat field, where the team will be focused on ensuring LAN communication signal error (e.g., latencies, signal connection) remains low in addition to LOS.	<ul style="list-style-type: none"> <li>• Wireless LAN communication tests with better connectivity as compared to wired connections</li> <li>• LOS error for all heliostat operational modes tested</li> <li>• Completion of the fiber optic network upgrades with no signal issues.</li> </ul>	<ul style="list-style-type: none"> <li>• &lt;1% RMS signal error</li> <li>• 0% LOS Error Validated</li> <li>• 100% Completion</li> </ul>	This work will be assessed for all primary NSTTF heliostat field operational modes, and against previous data sets. This will include multiple aim point strategies, and compared to the current three-wire communication controls setup as the baseline.	Required to ensure proper communications between the control room with all heliostats, to facilitate confident operations of the NSTTF solar tower facility.

### Milestone 1.2.1 – Protocol Development & Technical Down-Selections

For milestone 1.2.1, the team utilized the Table 3 assessment tool to track progress for the development of a new communication protocol library developed with LabVIEW 2023, that operates from the Host DSC to each remote Heliostat Servo Smart Drive. The team used the assessment tool to complete phased development of the FPGA with modularity validation, based on a protocol down selection that was facilitated based on commercial scale communication protocols. This down selection process consisted of assessment of potential candidate connections based on network software/hardware complexity and costs for either: Industrial Ethernet/CAT protocol, or B. RS232 (requires a RS232 to Ethernet Converter to pass the data to Network) connections. The team used the tool to also ensure that the network communication engine library was developed with the new software upgrades completed with QSMA principals from host to remote connections. This allowed the team to provide an NSTTF platform to have modularity of adapting the heliostat field to newer functionalities should future CSP customers require flexibility with respective installations.

**Table 3.** Milestone 1.2.1 Assessment Tool Excerpt

Description	Metric	Success Value	Assessment Tool	Metric Justification
The balance of system will be designed and fabricated within the SNL NSTTF 220' level. The team will complete a P&ID of system instrumentation and controls, along with subcomponent placements, positioning and mounting, as well as fabrication based on prior procurements. Initial testing of the flow lines will also take place to shake-down the BOS.	<ul style="list-style-type: none"> <li>• FPGA interface roadmap completed</li> <li>• Modularity validated with varying operational modes</li> <li>• Heliostat field utilization survey completed</li> <li>• Completion of network communication engine library with QMH protocols</li> <li>• Down-selection of an optimal communications protocol</li> <li>• Protocol with no interface issues between high-speed DAQ, slow-speed DAQ and site weather stations</li> </ul>	<ul style="list-style-type: none"> <li>• 100% complete</li> <li>• 100% validation completion</li> <li>• 100% complete</li> <li>• 100% complete</li> <li>• 100% complete</li> <li>• 100% completion with no issues found.</li> </ul>	The team will use existing protocols & wired hardware as the baseline for the NSTTF. The team will ensure that primary baseline nominal operational modes can be maintained.	Required to ensure proper controls and operations for the NSTTF solar tower facility.

### Milestone 1.2.2 – Final Controls Upgrades and Communications Validation

Finally, for milestone 1.2.2, the team utilized the Table 4 assessment tool to track the final deployments of newly-developed remote and host software, along with validation from Sandia LabVIEW experts during the final shake-downs. The assessment tool was used to track completions of final software/controls deployments, host interface development and data exchange performance between the host DSC computer and the PLCs, as well as flux testing on the solar tower. Here, the team leveraged this milestones assessment tool to perform flux biasing with heliostats with new software and perform communication signal final checkouts for each heliostat. Finally, the team used the assessment tool to track final field metrology on varying test bays of solar tower one. The team plans to complete flux measurement metrology for the G3P3 tower once its construction is completed.

**Table 4.** Milestone 1.2.1 Assessment Tool Excerpt

Description	Metric	Success Value	Assessment Tool	Metric Justification
<p>The final installed integrated controls will be assessed to ensure proper and confident functionality. It will also be assessed against the current NSTTF wired baseline controls and communication system.</p>	<ul style="list-style-type: none"> <li>• Successful final deployment of new software and controls</li> <li>• Successful deployment of the host interface</li> <li>• LOS during initial field operational modes testing between both interfaces</li> <li>• Validated physical network speeds</li> <li>• Data exchange between heliostats and host computer speeds</li> <li>• Local heliostat communication validated</li> <li>• Solar tower test bay DAQ systems upgraded for closed-loop controls capabilities</li> <li>• Complete field metrology for all upgraded heliostats (218) to optimize pointing</li> </ul>	<ul style="list-style-type: none"> <li>• 100% completion for all 218 heliostats.</li> <li>• 100% completion</li> <li>• 0% LOS detected</li> <li>• &gt;300 Mbps</li> <li>• &gt;300 Mbps</li> <li>• 100% completion</li> <li>• 100% completion</li> <li>• 100% completion for all 3 test bays</li> </ul>	<p>The team will need to ensure that the evaluation criteria is met to provide reliable heliostat field and DCS communication and control operations at the NSTTF. These criteria will be verified through electrical continuity testing with signal injection, and signal rate/quality confirmation using LabVIEW NI MAX. Metrology verification of control errors will be assessed through BCS characterization with HelioCon metrology group oversight.</p>	<p>Required to ensure proper controls and operations for the NSTTF solar tower facility.</p>

### 3. PROJECT OVERVIEW

For this project, an assessment of the current field of 218 Heliostats first considered the field asphalt, the structural members of the heliostats, the control system, the communications system, the drives, motors and encoders, and facet condition. The results of this assessments are as follows:

- The **structural aspects of the heliostats** remain sound. Visual assessments of the truss and torque tubes did not reveal excessive wear. The field has not experienced any failures of these structural components.
  - no action sought at this time.
- Surface inspection of **the foundations of each heliostat** also did not reveal cracking or degradation of the concrete, although we note without core sampling and analysis of the concrete it is not possible to estimate remaining life.
  - no action sought at this time.
- Assessment of the field **surface asphalt revealed that it is significantly worn**. The asphalt surface keeps the facets cleaner than a natural surface.
  - Estimates for replacement were over \$1M, deferred to a later date.
- The **heliostat facets** were found to be in good condition. A few of the mirrors have cracks or are broken. Minor corrosion of metal frames is evident. Spare frames are available; the mirrors were re-silvered in 2012.
  - no action sought at this time.
- The motors are replaced as needed. Encoders are working as expected. Both components will need to be updated in the future to newer models.
  - no action sought at this time.
- The original control system was deemed outdated, and components are unsupported and difficult to procure. The remainder of this proposal outlines two plans to update and refurbish the control system at the NSTTF to provide the reliability and functionality needed for future work including G3P3.
  - Refurbishment recommended and completed in this project
- Communications: The current Heliostat LAN was upgraded to Fiber optic lines (10 Gbps speeds) instead of PoE lines (2 Mbps). Currently 30% of the field has been upgraded to FO on previous funding.
  - no action needed.

#### 3.1 Status and limitations of current controls system, software and hardware

The NSTTF currently uses a LabVIEW software platform, where the code (Fig. 5) was developed by a third-party company (now out of business) over 14 years ago. This code was deemed outdated, where it supplied operational controls to provide signals for motion control of the 218 heliostats. The original controls hardware within the heliostat field, for each respective heliostat, consisted of an obsolete National Instruments (NI) real time controller (cRIO), model 9032. National Instruments does not maintain the current version of the cRIO where replacement or repairs would require upgrading the device to a newer model. Also, the current Elevation and Azimuth drive modules (NI 9505 Card) from National Instruments were also obsolete as well. Both modules during their time of deployment date back to 2005, which then were able to provide the motion to each respective azimuth and elevation axis motor, including each absolute encoder feedback signal. Since the NI modules are obsolete, National Instruments was not willing to guarantee any long life of the module to continue

its operations. With this current hardware, the NSTTF was only able to operate with LabVIEW version 2008, which has functionality limitations. These limitations included not having LabVIEW Event Functions, which would improve controls efficiencies within the controls code, for example. Additionally, the NI modules have the SSI feedback capability using the FPGA board functionality that only works using LabVIEW FPGA 2008, currently limiting control signal operations.

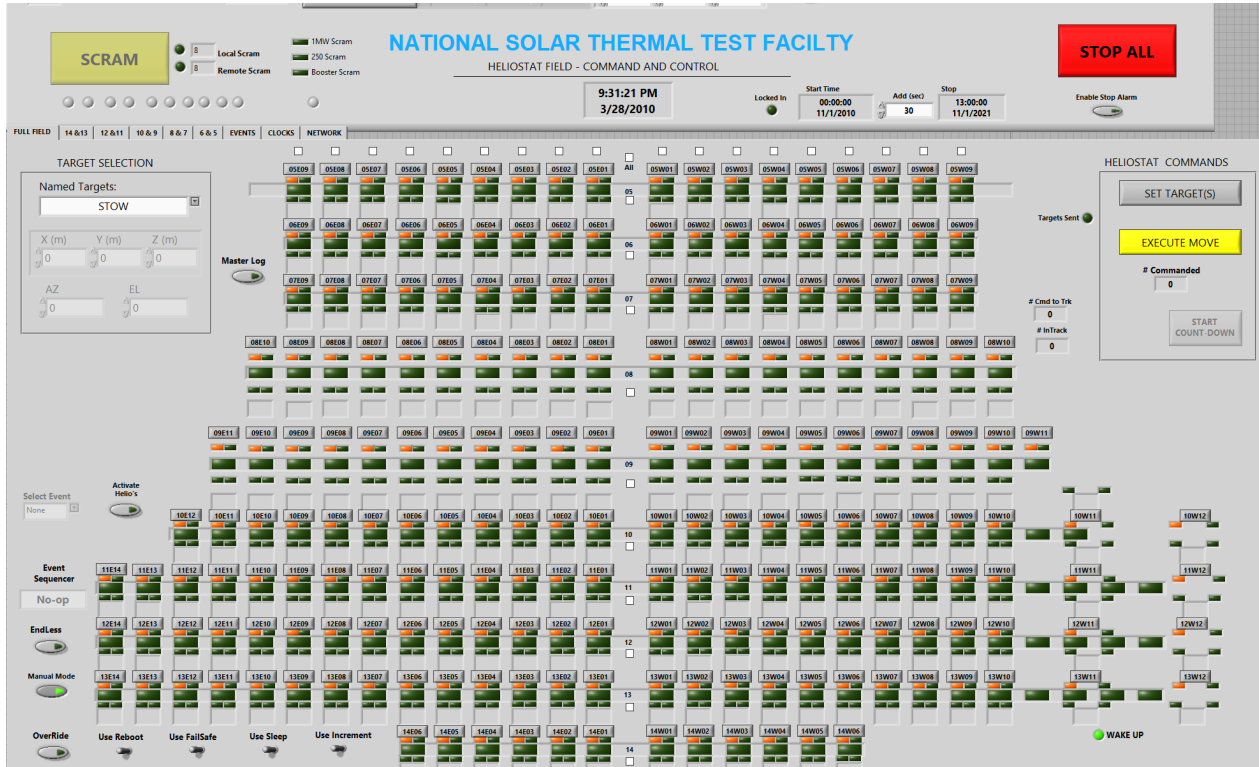
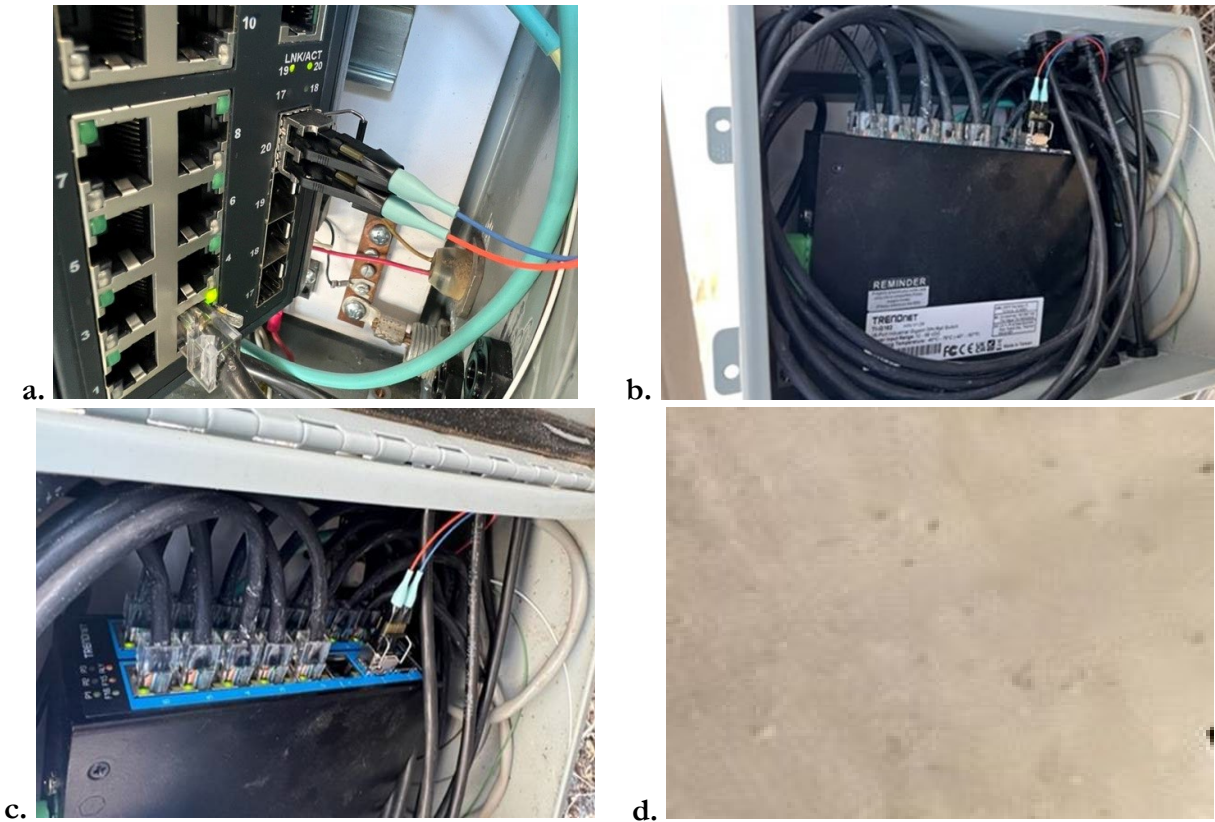


Figure 5. Control room LabVIEW code.

Most modern feedback motion hardware (if it would be upgraded) do not have the SSI type of feedback (like the original SNL NSTTF current absolute encoders have from each heliostat), instead they either have modern types of feedback like Sine-Cosine, Quadrature, Absolute Encoders, etc.

Another constraint identified was that the host side of the software was written in LabVIEW 2008 from almost 15 years ago. For this effort, the team utilized DOE funding to also upgrade the host side of the software within the Heliostat Operator computer, located in the NSTTF control room. This has allowed faster communications with each heliostat and has avoided detrimental network drops that occur during testing, which will reduce testing delays and schedule critical path project issues that have occurred over the last 10 years. The host side of the software that controls each heliostat was written in LabVIEW 8.6 which originally lacked modern features (of the newer versions like LabVIEW 2023) such as clear variant data path, multi-error support, etc., which are reliable to develop a modern controls software. The work performed in this effort facilitated upgrades to the current controls hardware and software of the NSTTF to more modernize the operating motion controls that can satisfy state-of-the-art needs of NSTTF customers, DOE SETO program, and the CSP industry for at least 25 years. This work was facilitated in parallel with the software development phases.





**Figure 7.** Heliostat field fiber optic cabling connections.

#### **4.1.2 Software Development**

The team revised the current software architecture (Figure 8) of the system to upgrade the software in a timely manner to meet the project end date goals. The current Sun Tracking algorithm was found to be outdated and complex. The team began this effort by revising five algorithms from the Italian Solar Radiation Atlas, their algorithms have a maximum error of 0.003 deg. The team created a data set of the month of June using the five algorithms and compare the data collected to the Sun Calculator organization for validation.

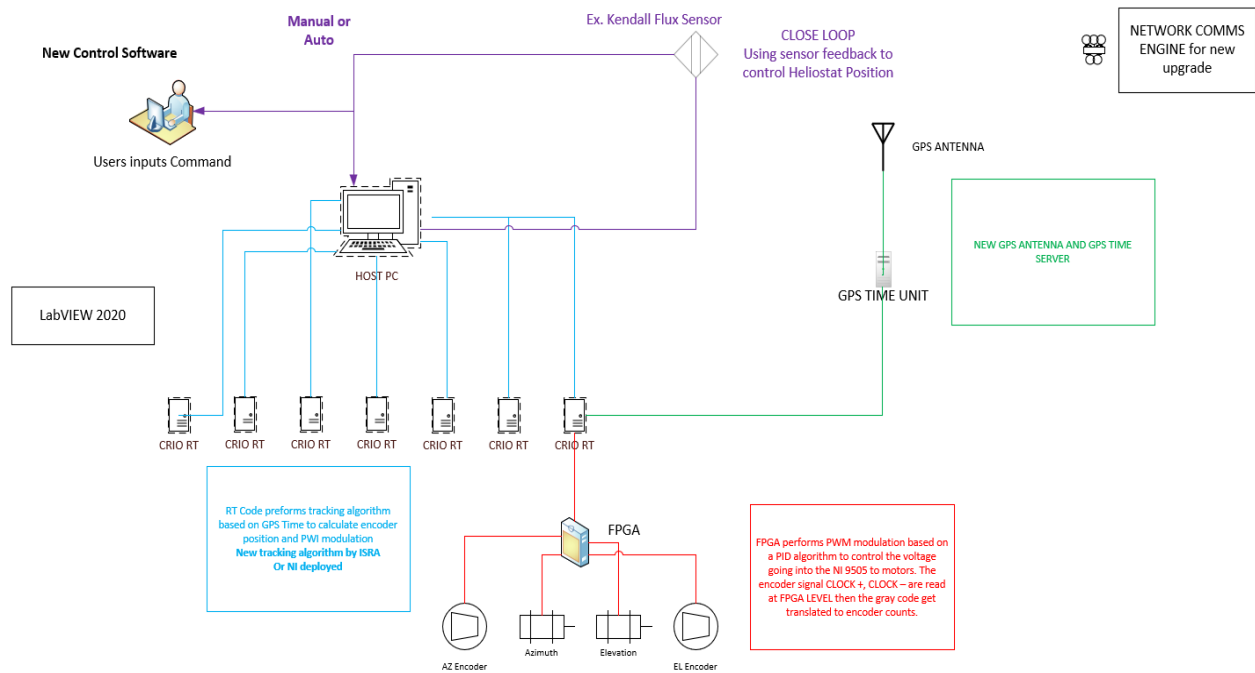


**Figure 8.** FPGA software development architecture.

The team updated the field programmable arrays (FPGA) interface, real-time (RT) interface, and Host interface. Members of the SNL Group 7661 assisted in developing the software, supervised by the NSTTF team. Mike Sibley led the development of the FPGA interface, with consultation through Lonnie Haden and Luis Garcia Maldonado. Figure 9 shows the new NSTTF Heliostat Field Control Software System Tree with all the new capabilities including Closed Loop Control. This logic will allow signal checks as well as an architecture that the team can later evaluate cyber security aspects related to heliostat field operations. The green processes illustrated under the Closed Loop sub-interface adds the capability of a hybrid system. Currently the system only allows for manual aim pointing with the operator input. With this new control software, the operator can enable one of the five closed loop algorithms to track efficiently onto a desired target. This software development was a major focus for the early stages of the refurbishment project as the FPGA interface allows for communication between the updated cRIO 9053 chassis and the NI 9505 modules; this permits azimuth and elevation angle operations and simulations to occur. The completion of the FPGA interface allows the team to bench test closed loop control software in tandem with the FPGA interface code as well as testing and integration with wireless communication. The RT interface contains extra modules and connections to interact with the FPGA interface to provide the ability to smoothly integrate different closed loop control codes for testing and validation on the heliostat field.

## NSTTF HELIOSTAT CONTROL SYSTEM TREE

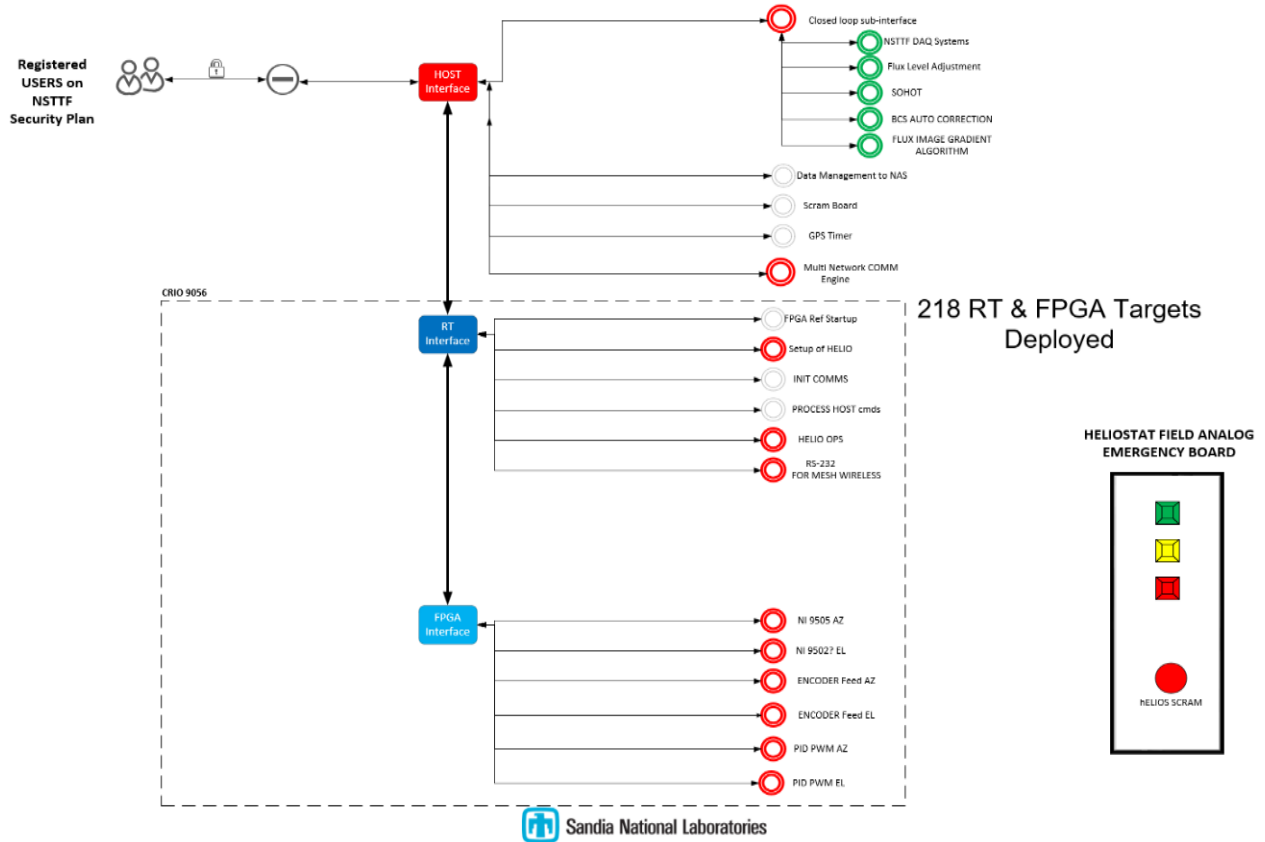


**Figure 9.** NSTTF Heliostat Field Control Software Architecture.

The overall new software architecture uses LabVIEW 20.0 and utilizes Windows 10 as a standalone system to help avoid cyber security issues. The field also retains its hardline for the current 218 heliostats for SCRAM operations, though any additional heliostats that are added will require a hardline connection for SCRAM as well, in addition to the wireless communications. Figures 10 and 11 provide details that were followed for this subtask both in terms of work breakdown and timeline. The three subtasks that were facilitated for this software development were: FPGA, RT and Host Interface software development.

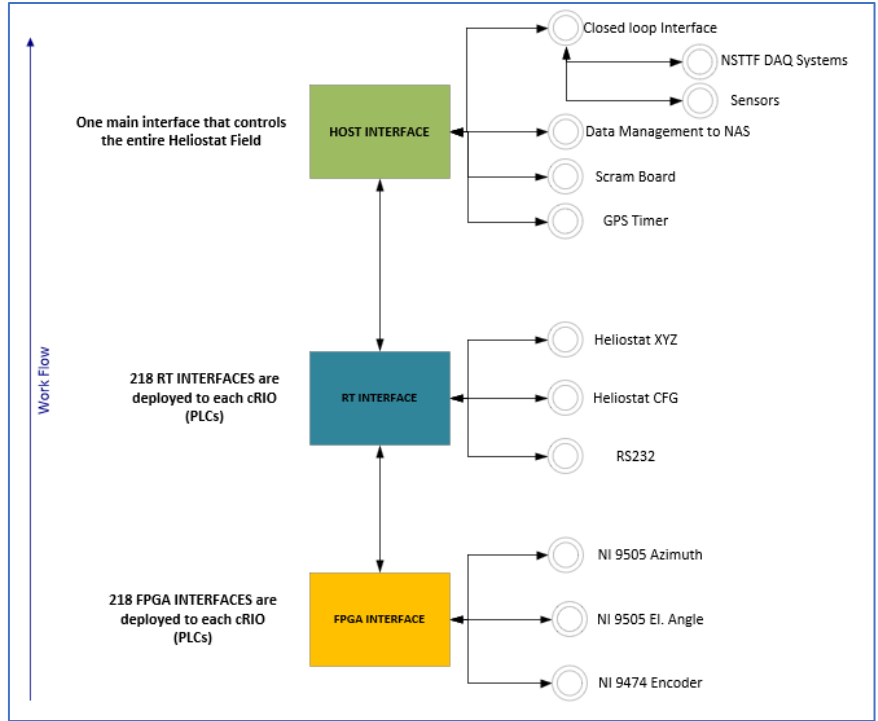


**Figure 10. 3 HelioStat Software Control System Breakdown**

Task Name
<b>Host Interface</b>
Data Fast DAQ on Tower
Data Slow DAQ on Tower
Modular Customer DAQ
Modular Customer Sensors
BCS Camera
DNI
Wind
Weather
GPS Timer
Logging Data (At 5 second)
Simulation Test
Validate Software
API
NAS
Data Mgmt
Scram Board
Utility VI's

Task Name
<b>FPGA Interface</b>
NI 9505 Azimuth
NI 9505 El. Angle
NI 9474 SSI Encoder
Test Interface
Simulation (Install into 9503 Tester)
Validate FPGA

Task Name
<b>RT Interface</b>
Talk with FPGA Interface
Perform Tracking Calculation
Extra Connection
Extra Modules
RS-232 (SD)
Develop Intermediate Programs
Heliostat CFG
Tower Bound
Heliostat XYZ
Simulation Test
Validate RT

**Figure 11.** Software architecture subtasks and development work breakdown.

During development, the Heliostat Engine had multiple checks completed to ensure it had the correct update indicators in each corner of the engine. This provides the heliostat operator feedback about the Heliostat motion (in elevation and Azimuth axis), it provided tracking information (if the heliostat started tracking in the desired position), Network communications (this provided an indication if the RT target or PLC is online and responsive), lastly, we have the SLEEP indicator that notifies the heliostat operator about status of the PLC chassis.

Another feature of the Heliostat Engine is the reset of encoders. This functionality gives the operator the ability to perform a power cycle on both azimuth and elevation encoders in case of error. FPGA errors reporting is now included in the Heliostat Engine providing the more reliability of the execution of motors movements. The following is a short timeline detailing steps taken in the software checkouts process:

GPS timer hardware was tested with 1 single engine and tested over a period of 7 days. During the final deployment of the cRIOs into heliostats, the GPS antenna will be installed, and the unit will be recording 24/7 GPS time.

EVENTS: this primary functionality was built and deployed into the HOST software. This was an old feature of the current control software that helps with CSP receiver testing, AirForce Testing, and Aerospace testing at the current NSTTF Solar Tower. This functionality gives you an easy modular sub-set movement of heliostat into a desired [XYZ] tower coordinate.

Prior to heliostat field testing the ID's of the heliostat were identified initially. The new cRIOs initially presented many errors with the old control software, so careful testing with the new control software was necessary to refine the functionality and see if the errors were removed from the motion of the motors. Also, the test was performed at certain local coordinates of the NSTTF Tower, where previous test showed errors with the current heliostat software. Once the testing was completed, the final deployment of the new cRIO controllers was planned. The deployment of the new cRIOs took approximately 2 weeks for installation and powering/electrical work. By the end of deployment, the new HOST control software was online to operate the Heliostat Field. Additionally, a code refactoring was done to address any misused section of the code or debugging blocks that need to be removed and maintain a generic architecture for future development. This gave the team the opportunity to add new functionalities to the controlling of the Heliostat Field System, this includes closed loop controls algorithms adaptations and wireless communications implementation. After the completion

of the new cRIO hardware installation into the field, the focus turned to updating the cRIOs with the new RT code. Each cRIO's individual IP was synced to allow RT updates not occur in the control room from the new control room computer station.

As shown in Figure 12, to allow for continuous heliostat checkout testing within the heliostat field, the team initially refined the current code to be operated in a much more efficient manner, particularly with respect to the on-board cRIO firmware. This has allowed for faster more reliable operation, and the ability to make changes much easier in the future. The team initially focused on the development of the queue state machine (QSMA) as well as the interface of the FPGA with the RT software codes. The team also started validation testing with regard to angle position transfer functions and sun position algorithms for open-loop controls.

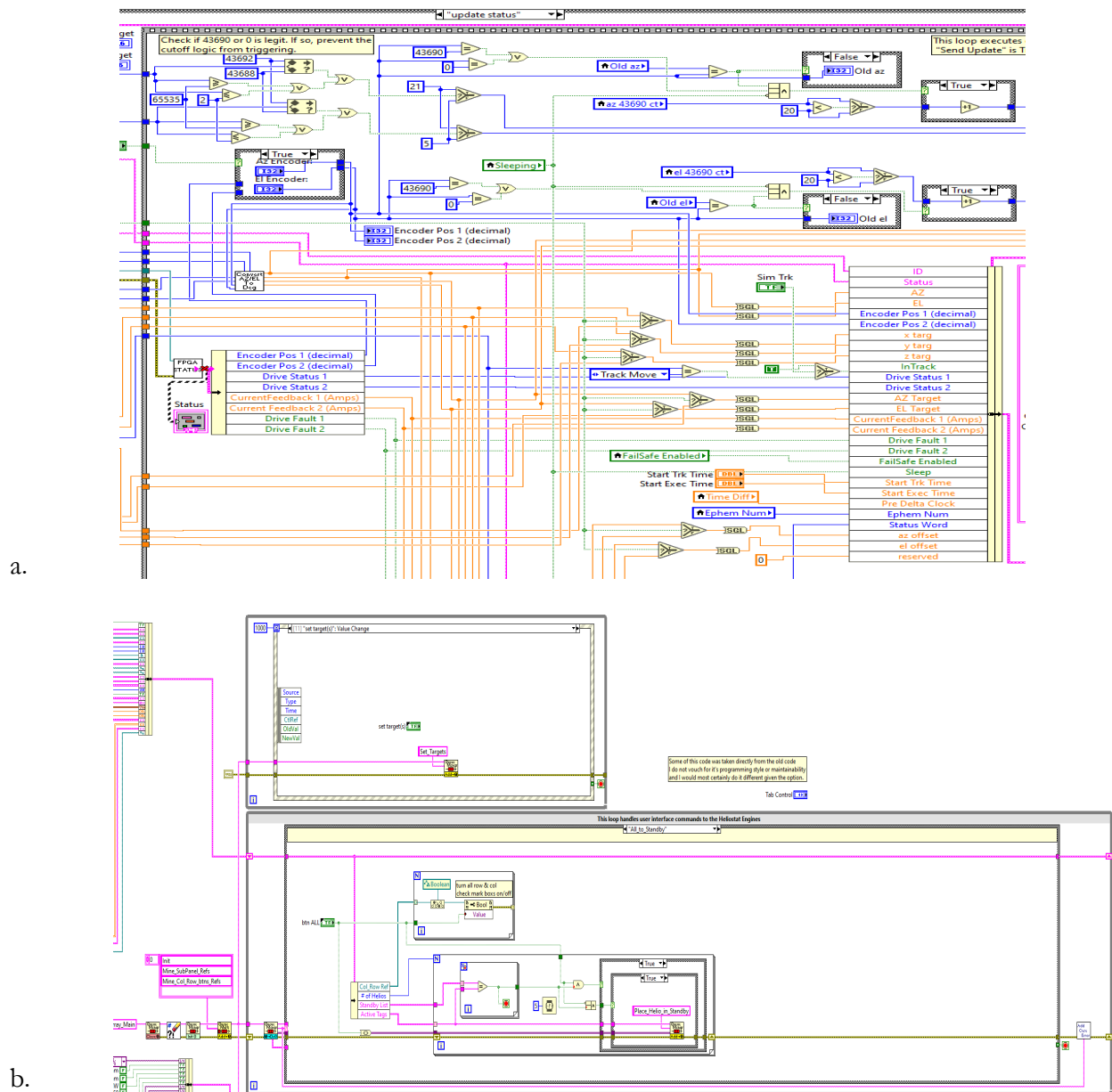
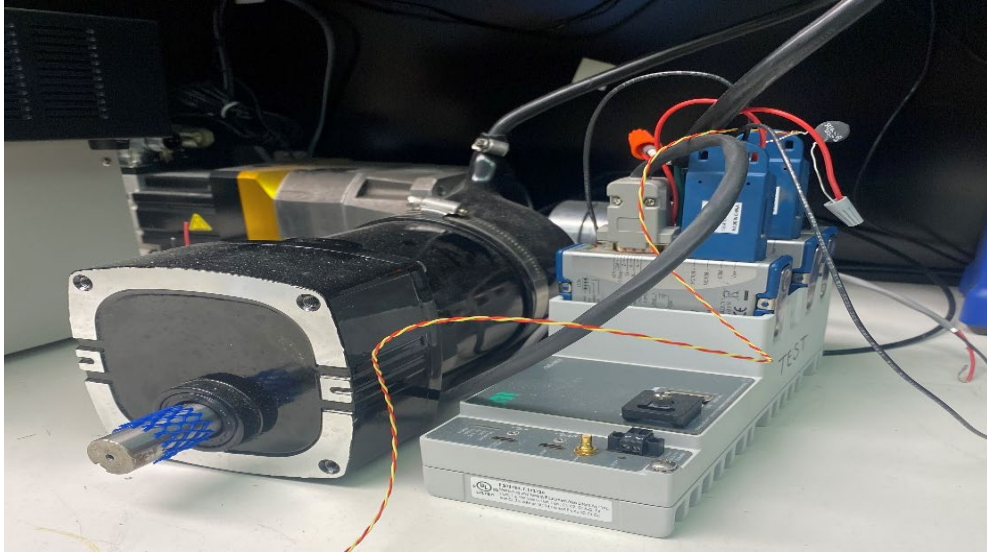


Figure 12. a. Old NSTTF FPGA code and b. new NSTTF FPGA code example.

During the later phases of the project the team uploaded maturing versions of the RT code for all 218 cRIOs in addition to the latest OS system installation. Each unit required a discrete operating system to run the azimuth and elevation angle drives. From installation, the software development team deployed and tested new c-RIOs with a direct current (DC) brushless motor under clockwise and counterclockwise directions, and monitored amperage draw and stability shown in Figure 13.



**Figure 13.** The current axis DC brushless motor with new Real Time Controller testing motion control

Preliminary testing was successful at moving two small DC motors using the c-RIOs along with the motion control modules and the current Real-Time software. These two sub-systems were then tested with a Knocker setup at the 200-foot level in the tower (Figure 14). Power to the Knocker setup was altered to 120V from 480V (Figure 15) to allow for more efficient and higher frequency testing. This setup includes two full axes with encoders allowing the software development team to test the FPGA and Real Time software with real hardware and evaluate the code. Extensive testing of the newly built FPGA software was completed using the new host interface to control the azimuth and elevation angle motors. Through the host GUI, the team was able to move both the azimuth motor and elevation angle motor in both directions with complete accuracy in reference to the encoder.

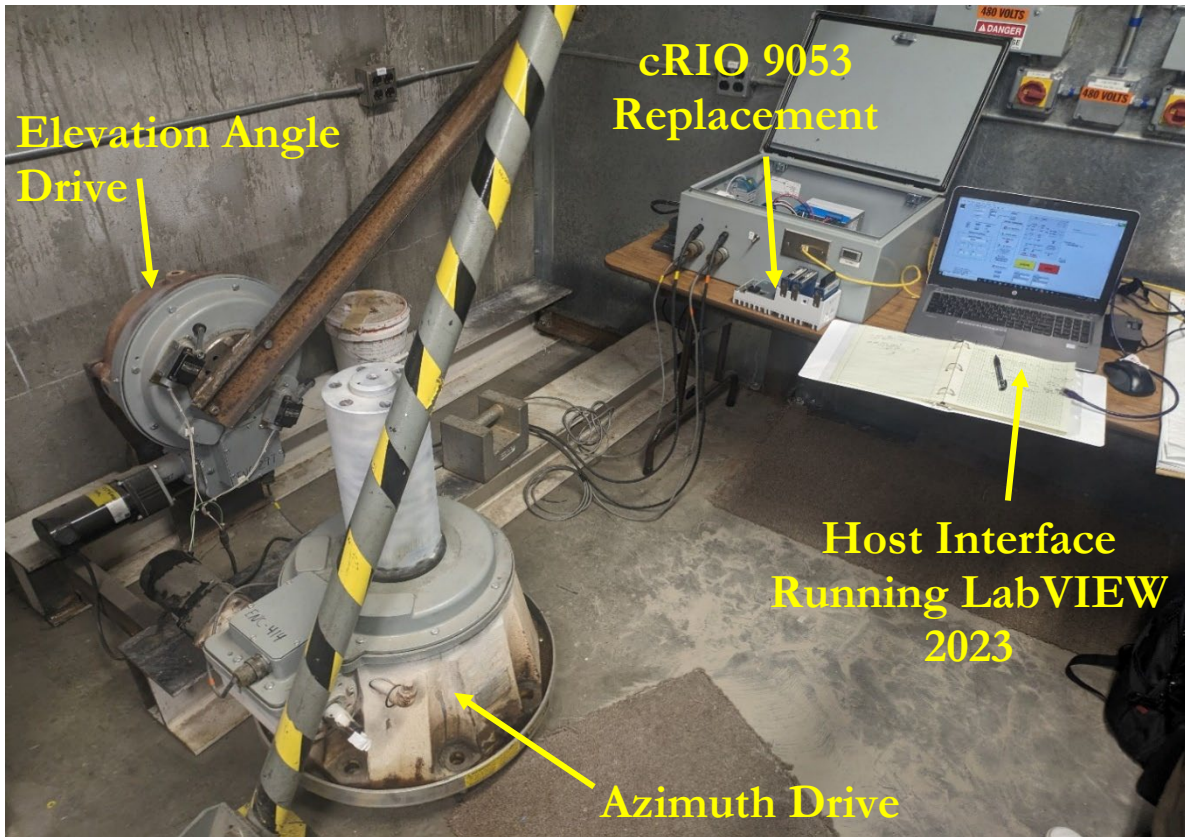


Figure 14. Knocker Setup with Two-Axis Elevation and Azimuth.

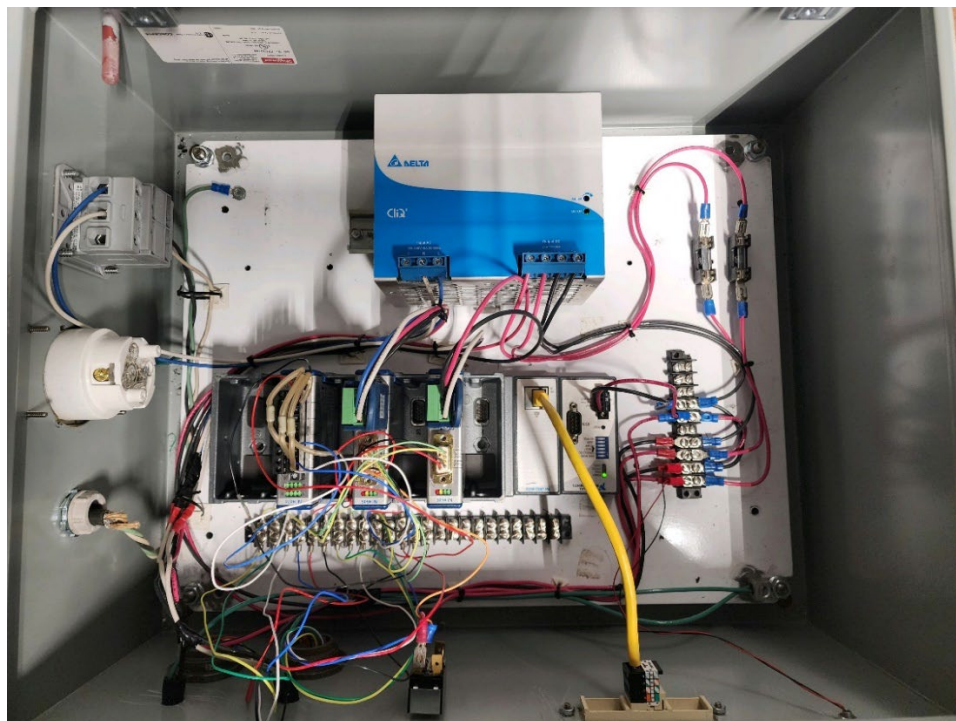


Figure 15. Knocker Setup Enclosure Voltage Downgraded to 120V.

The Real Time sub-system included the new sun tracking algorithm to obtain a sun tracking position error of less than 0.5 mrad. The HOST sub-system running the entire system was tested using simulated data to launch Heliostat RT. The c-RIO RT software was rewritten and placed into an architecture that will make the code easier to understand and much more maintainable in the future. The RT software was by far the most involved portion of the software development, where decoding the legacy software was found to be time consuming. The GUI software was also rewritten and placed into an architecture that made the code easier to understand and much more maintainable in the future. The initial layout of the GUI elements was completed including implementing a few changes based on operator feedback (Figure 16).

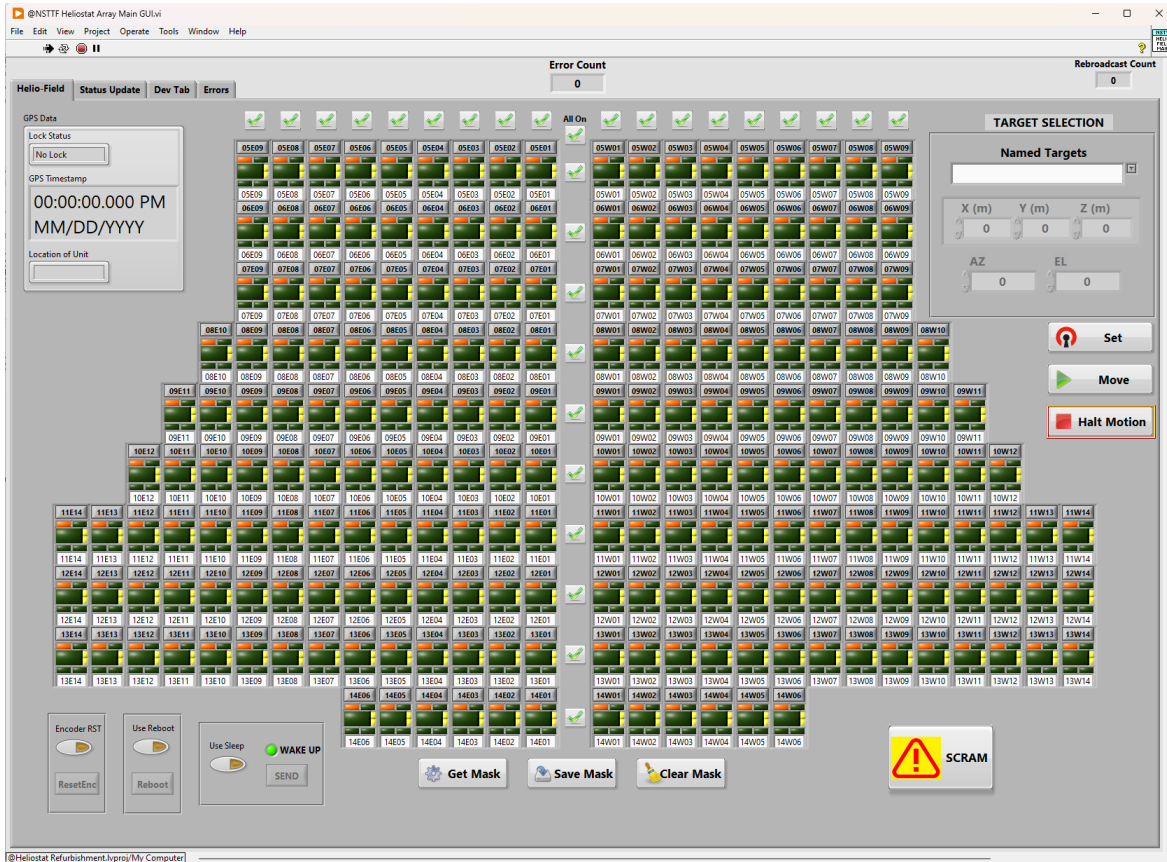


Figure 1. NSTTF Heliostat Field GUI.

At the end of the project, the FPGA and RT development was completed, in addition to networking and integration of the NAS. Here, the SNL team completed extensive field testing of the new FPGA and Real Time portions of the code have been completed, initially using a single heliostat to gain validation of functionality. The new DSC was built and tested with LabVIEW 2023 version and the GPS timer hardware was installed. Calibrations to increase the overall potential field flux levels were also undertaken by utilizing the BCS target. Each heliostat in the field was individually brought onto the BCS target using the new GPS timer tracking system to find any beam offsets caused by inaccuracies through the encoders, GPS marked locations for said heliostats, or wear on the azimuth and elevation angle gearing.

#### 4.1.3 cRIO Programmable Logic Controller (PLC) Upgrades

Early in the project, National Instruments (NI) achieved their delivery goal, and the NSTTF received

all 218 CRIO 9053 in a timely manner. All the cRIOs were checked following Sandia Policy of Quality Level 2, Figure 17. This level inspects the purchased item in terms of physical appearance to confirm the item is received as described. The cRIOs were also logged into the SNL MAXIMO database file to keep an organized inventory. Each cRIO was assigned to a specific heliostat in the field. The cRIOs all had necessary drivers installed for the application of use in the heliostat field.



**Figure 17.** cRIO setup platform for installing software and wireless hardware.

#### **4.1.3 Heliostat Field Wireless Communications Upgrades**

The team also facilitated the wireless implementation portion of the Heliostat Refurbishment Project. Initially, equipment to build out 16 heliostats with wireless controls for validation testing and confirmation of equipment functionality prior to a system-wide rollout was done early in the project. The team had to submit an internal SNL RTWI form to establish Wireless communication protocols on Sandia Enterprises systems. The team received a new GPS server and antenna, which allowed for better optimized sun tracking as the current GPS server is an outdated 1995 model. The GPS server (Figure 18) was originally tested with a small DAQ system to record data for 7 full days to validate the functionality and accuracy of the updated GPS time data.



**Figure 18.** New GPS Server for Sun Position Tracking Implementation

Initial testing of the new GPS timer using a novel software system allowed for much tighter sun tracking tolerancing than previously achievable with the outdated GPS system currently being used at the NSTTF. Figure 19 presents the original test setup for the simple testing stage of the GPS timer. The hardware open-loop controls code for the GPS timer was updated to the current NSTTF version of 2023 LabVIEW. To assess the validation of this system, Figure 20 shows the GUI interface developed at the NSTTF for software testing.



**Figure 19.** New GPS Timer Hardware where the antenna is located within the red circle.

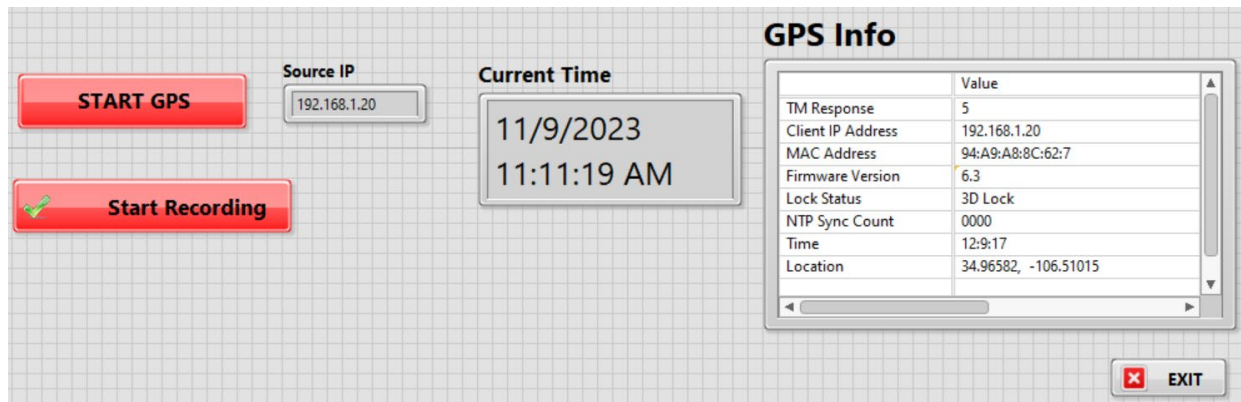


**Figure 20.** GUI for Validation of GPS System.

The communications at the SNL NSTT operated using ethernet comms, where Table 1 shows real time data of the performance of the new GPS timer with the upgraded Firmware version 6.3.

**Table 1.** Recorded Data from GPS Timer Testing

Time Elapsed since GPS start	Response Value	Client IP	MAC Address	Firmware Version
5	5	192.168.1.20	94:A9:A8:8C:62:7	6.3
10	5	192.168.1.20	94:A9:A8:8C:62:7	6.3
15	5	192.168.1.20	94:A9:A8:8C:62:7	6.3

Lock Status	NTP Sync Count	Time	Latitude	Longitude
3D Lock	0	14:18:45	34.96571	-106.51015
3D Lock	0	14:18:50	34.96571	-106.51015
3D Lock	0	14:18:55	34.96571	-106.51015

The team developed and tested DSC code to allow flexible interchange between communication types, which can also allow for security test changes, that can cycle between DOE and more sensitive DOD projects, for example. Figure 21 shows the bench top test bed of the wireless modules where the inner computer provided communication signals and the outer computers represent the heliostat receivers.



**Figure 21.** Wireless benchtop test setup for software and signal assessments with controller.

At the end of the project, Sandia Cyber security, completed RTWI approval to allow NSTTF WLAN with 16 access points and communications with wireless extenders and multi-connection antennas. For wifi, three primary END point wireless routers were deployed across the heliostat field to allow strong signal connectivity for all 218 heliostats. The team believed that this type of communication architecture could also be scalable, pending validation of the system at the NSTTF. Initially, the team also completed its received signal strength indicator (RSSI) signal tests in the heliostat field, as a preliminary means for measuring and evaluating signal strength and quality. Examples of these tests are shown in Figures 22 and 23, evaluating signal quality/strength with respect to communication direction.

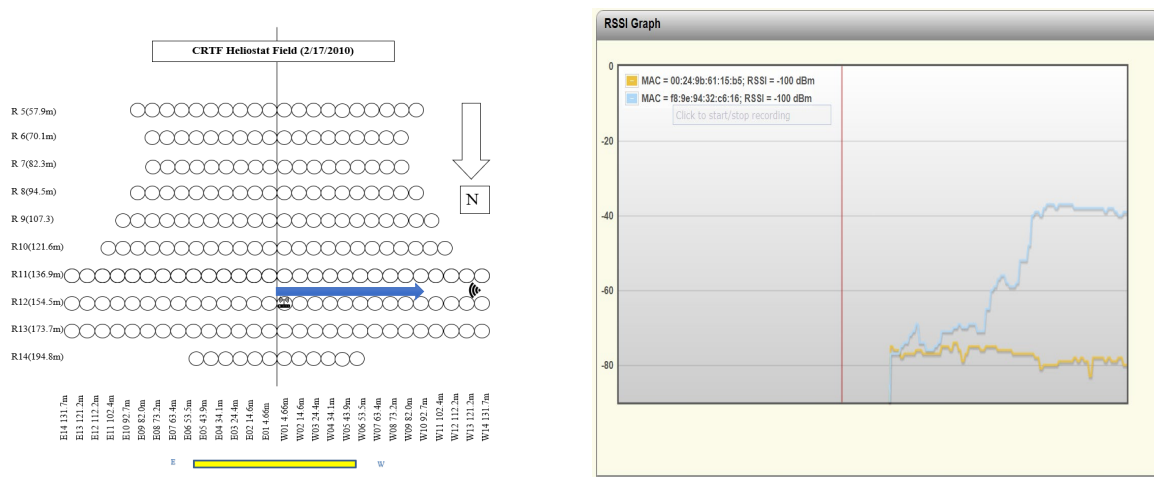


**Figure 22.** NSTTF Heliostat Field Eastward Wifi test initial results.

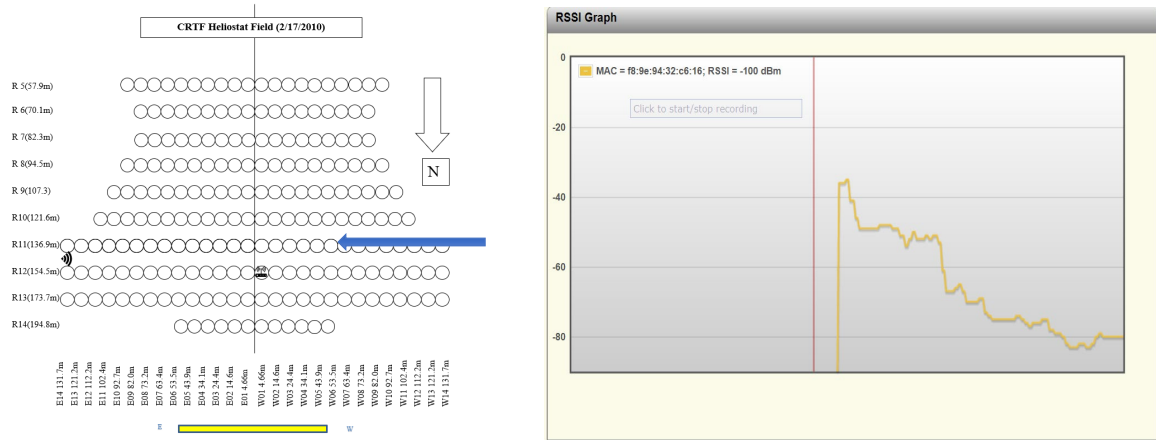


**Figure 23.** NSTTF Heliostat Field Westward Wifi test initial results.

The team facilitated additional benchtop testing for the 2.4 GHz Phoenix Contact wireless modules to verify functionality of using a pseudo-mesh network. Two wireless module types were setup to be deployed into the field: each heliostat will use a Phoenix Contact 1100 module to relay the signal to a Phoenix Contact 2100 which acted as an access point. The Phoenix Contact 2100 allows for communications between 60 unique signals. Six Phoenix Contact 2100 modules were placed at strategic locations throughout the field (Figure 24). Each Phoenix Contact 2100 will relay 36 individual Phoenix Contact 1100 heliostat signals for full heliostat field coverage. The pseudo-mesh signals will be transmitted to the in-field UISP airMAX 2.4 GHz antenna. Six 1100 modules connecting to one 2100 module were used in the successful benchtop testing, shown in Figure 25.

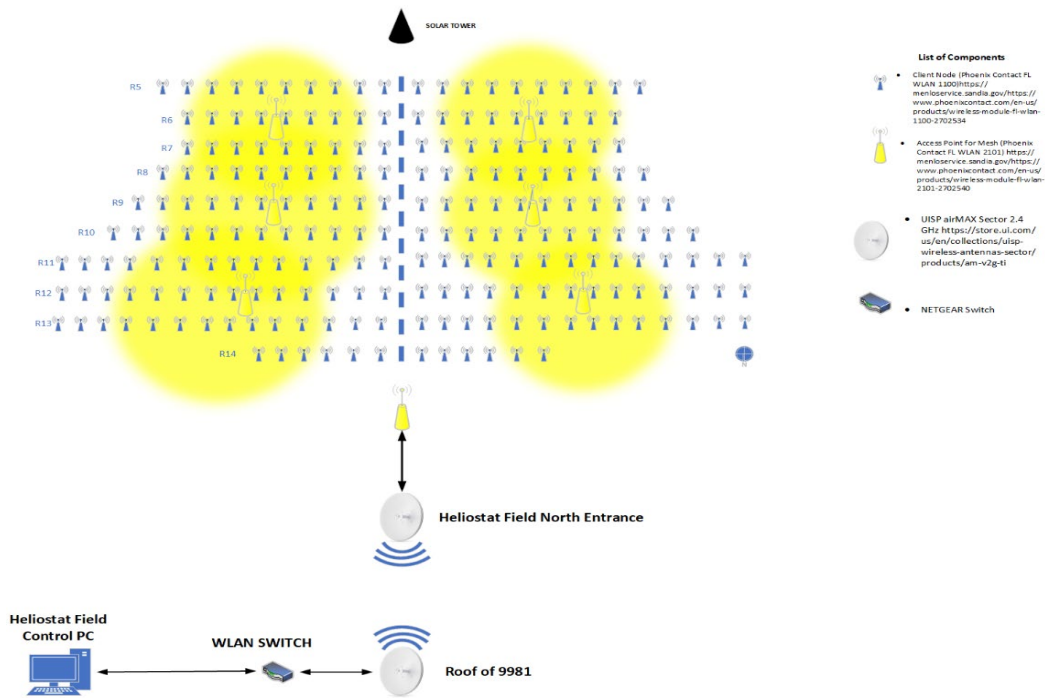


**Figure 24.** NSTTF Heliostat Field WLAN.



**Figure 24.** Benchtop Testing of Phoenix Contact 1100's and 2100 Pseudo-Mesh.

Field tests were also completed to test the signal quality of the UISP airMAX 2.4 GHz antennas. These antennas were used as the bridge between the control tower and the Phoenix Contact 2100 modules in the heliostat field. The initial field tests were run from ground level, placing the field antenna at the transformer station East of the heliostat field and installing the control room antenna at the SWEPT lab (Figure 25). The SWEPT lab was used as the comms station, imitating the control room, with the antenna hooking up to the TP-Link AXE5400 Wifi router purchased for the updated control room, seen in Figure 5. The locations for the antenna were chosen to maximize distance between them to show effects on signal quality. They were both kept at ground level to see how foliage, structures, and barriers effect signal strength.



**Figure 25.** Communications Station Antenna.

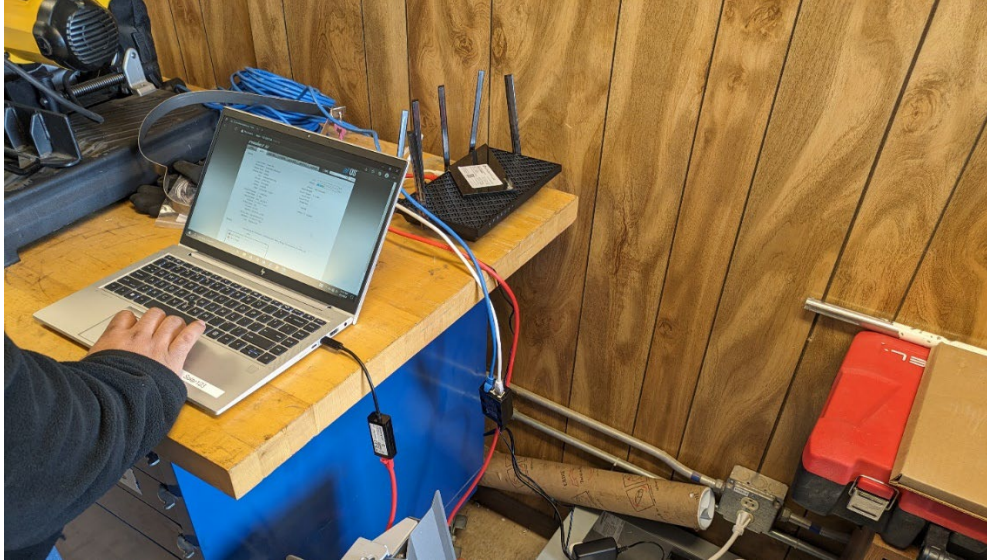


**Figure 26.** SWEPT Lab Comms Station with TP-Link AXE5400 Wireless Router.

Figure 27 shows the locations of the antennas, with the estimated 460-meter distance between the two antennas. The field antenna can be seen in Figures 28 and 29, along with the heliostats in the background disrupting line-of sight to the host antenna. Multiple tests were completed to show variation of signal quality with changes in orientation of the tower antenna. Figures 30 and 31 display the data collected from these initial tests, which includes the received signal strength at the comms station, and the signal strength of the transmitted signal from the comms station. The graphs read left to right, with the initial readings (in blue) having the antennas directly facing each other. The second set of readings, shown in purple, are the signal strength with the tower antenna rotated 90 degrees from the comms station antenna. The yellow readings had the tower antenna oriented 180 degrees from the comms station. The red datapoints had the tower antenna oriented downward and placed on the ground. The following four data points reoriented the antennas to directly face one another.

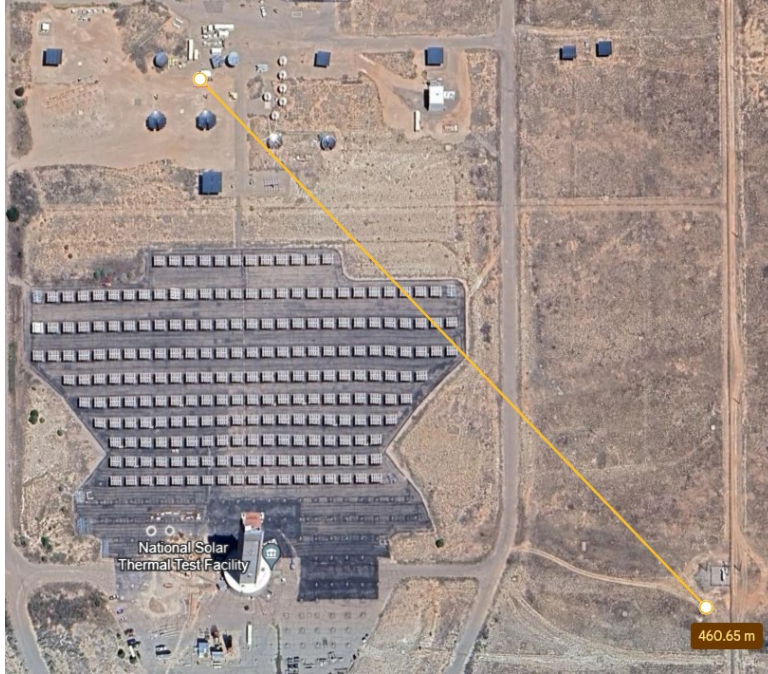


**Figure 28.** Antenna Locations at the NSTTF.



**Figure 29.** Field Antenna Testing.

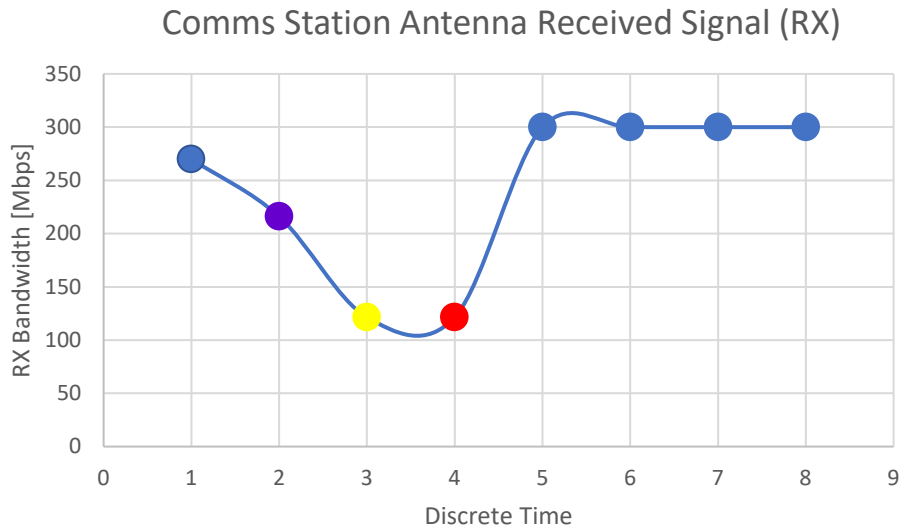


**Figure 30.** Comms Station Antenna Received Signal (RX).

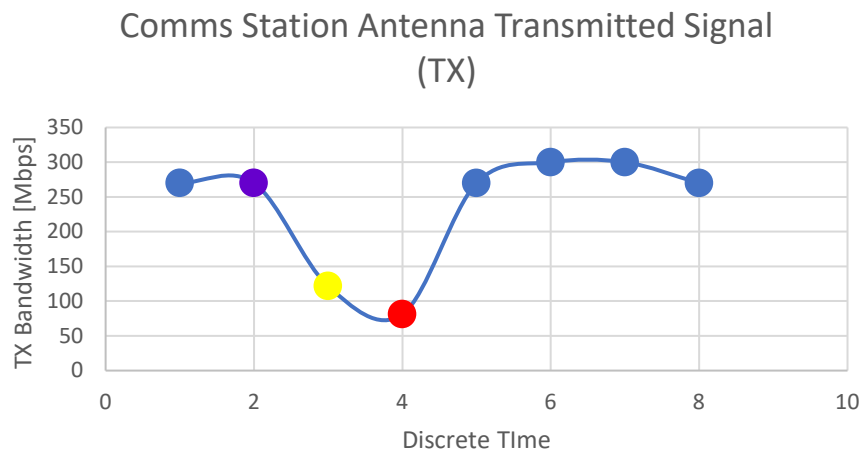


**Figure 31.** Comms Station Antenna Transmitted Signal (TX).

Following successful testing of the antennas, the team combined the Phoenix Contact wireless modules and the antennas to prove functionality of the entire Wi-Fi system. 2 Phoenix Contact 1100 modules were paired to one Phoenix Contact 2100 module (Figure 32), which relayed the signal to the field antenna. The field antenna then sent the signal to the control room antenna. The Phoenix Contact 1100's were placed at heliostats 12E3 and 12W3, with the Phoenix Contact 2100 at the center of row 12 (partially seen in Figure 33). Signal quality between the antennas was tested with rows 13 and 14 in “face south” position for increased potential signal disruption. Figures 34 and 35 show the Control Room Antenna GUI displaying data transfer from the field antenna. The test was successful, with data transmission from the Phoenix Contact 1100 modules being received at the control room antenna.

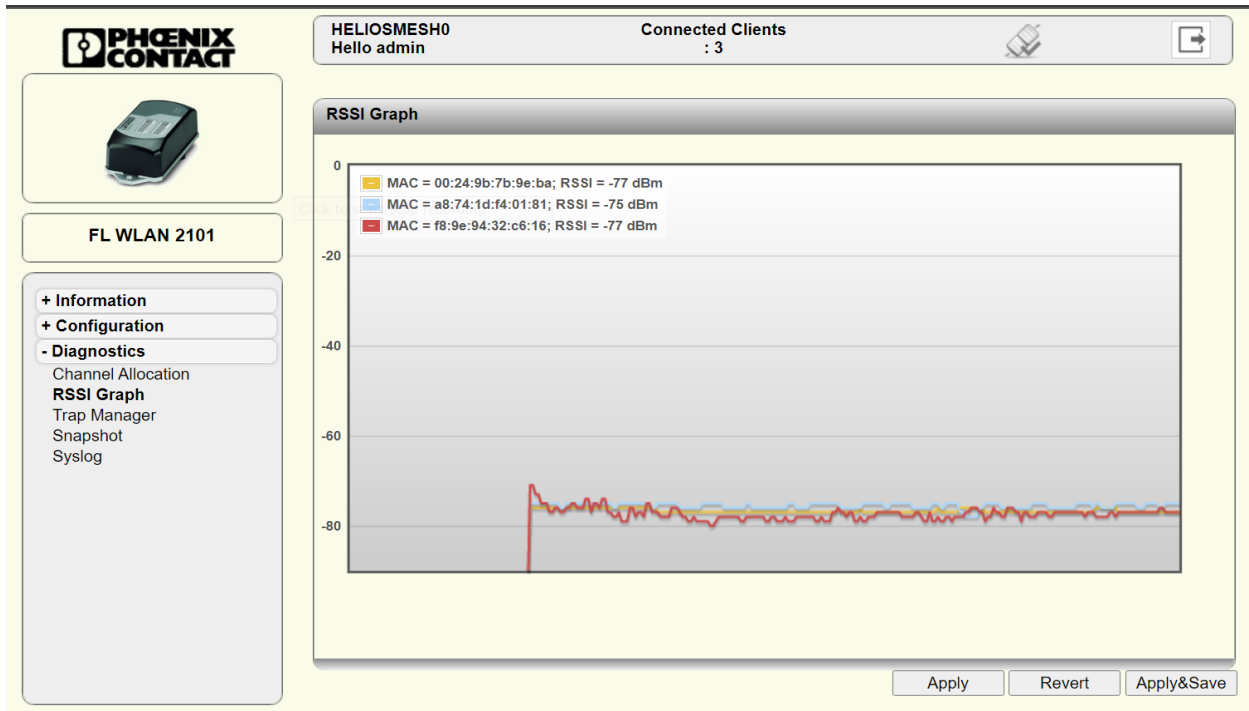


Figure 32. Successful Connection of 2 Phoenix Contact 1100's to the Phoenix Contact 2100.



Figure 33. Partial View of Module and Antenna System Test.

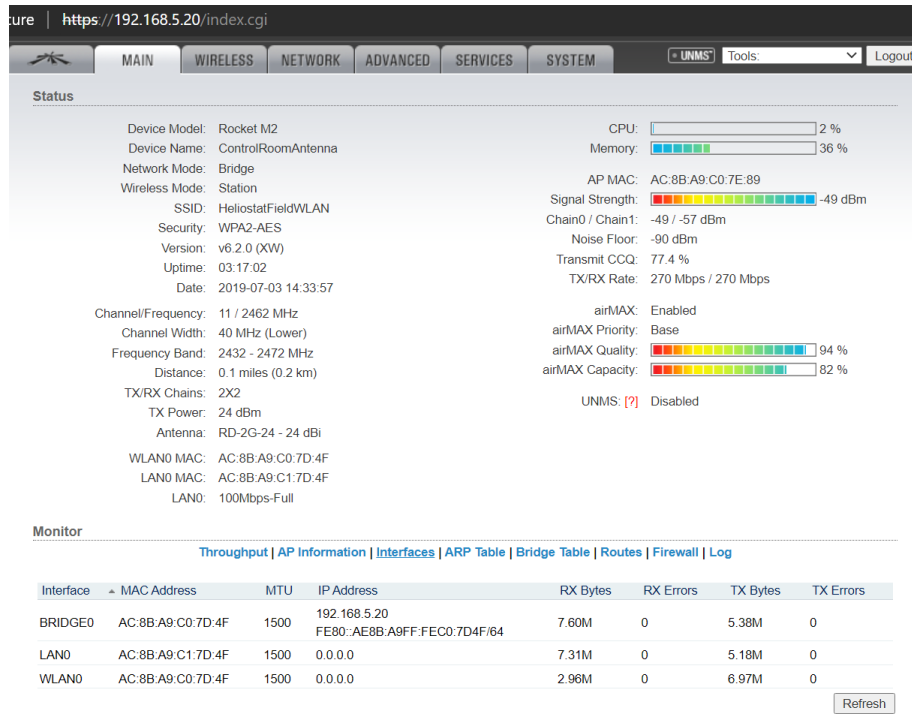


Figure 34. Control Room Antenna GUI With Connections and Signal Strength Displayed.

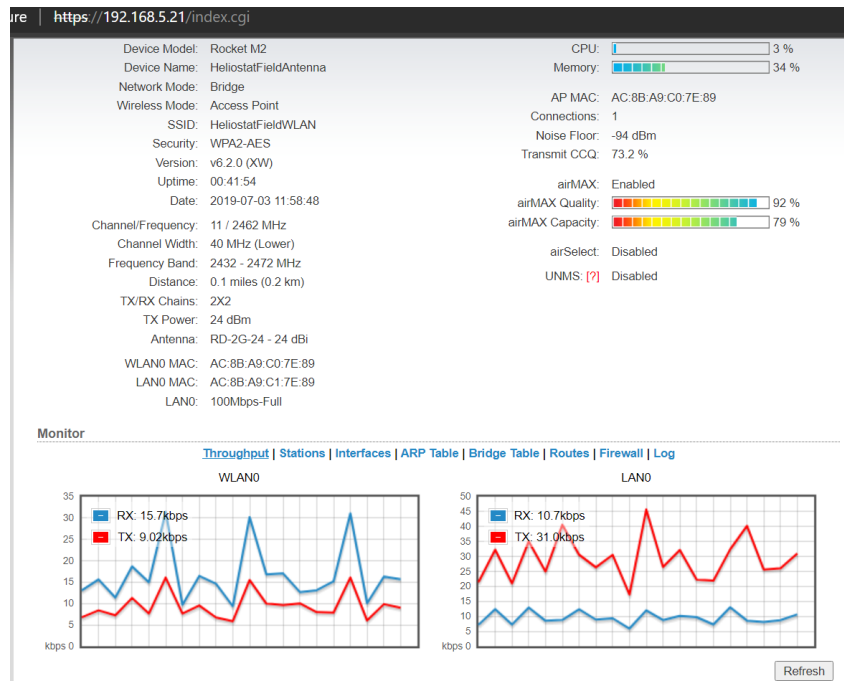


Figure 35. Control Room Antenna Real Time Signal.

With the successful Wi-Fi combined system field tests, the control room antenna was moved to its permanent location, atop the control room (Figure 36). This has allowed for continual Wi-Fi tests to be performed inside the control room tower, enabling the most accurate representation of how the system will be run during regular heliostat operations.



Figure 36. Control Room Antenna Permanent Location.

Extensive work was completed at the end of the project to validate reliable operation of the wireless system. The deployment of Wavelink AC12007 signal repeaters were field tested to guarantee strong signal strength to all heliostats in the field. showcases the field planned layout, with six zones sending their Wi-Fi signals to a centralized Wavelink AC12007. This repeater then transmits these zoned signals to the centralized Wavelink AX1800 repeater at the northern end of the tower, which in turn uses the airMAX Rocket Prism 2AC to relay the signals to the control room. This is represented in Figure 37. Testing was completed from the control room using this configuration to see signal latency. In an attempt to distort the signal, the heliostats were oriented to face due south to minimize line-of-sight for all hardware involved. Figures 38 and 39 show the successful data transfer of 50 packets with no data lost.

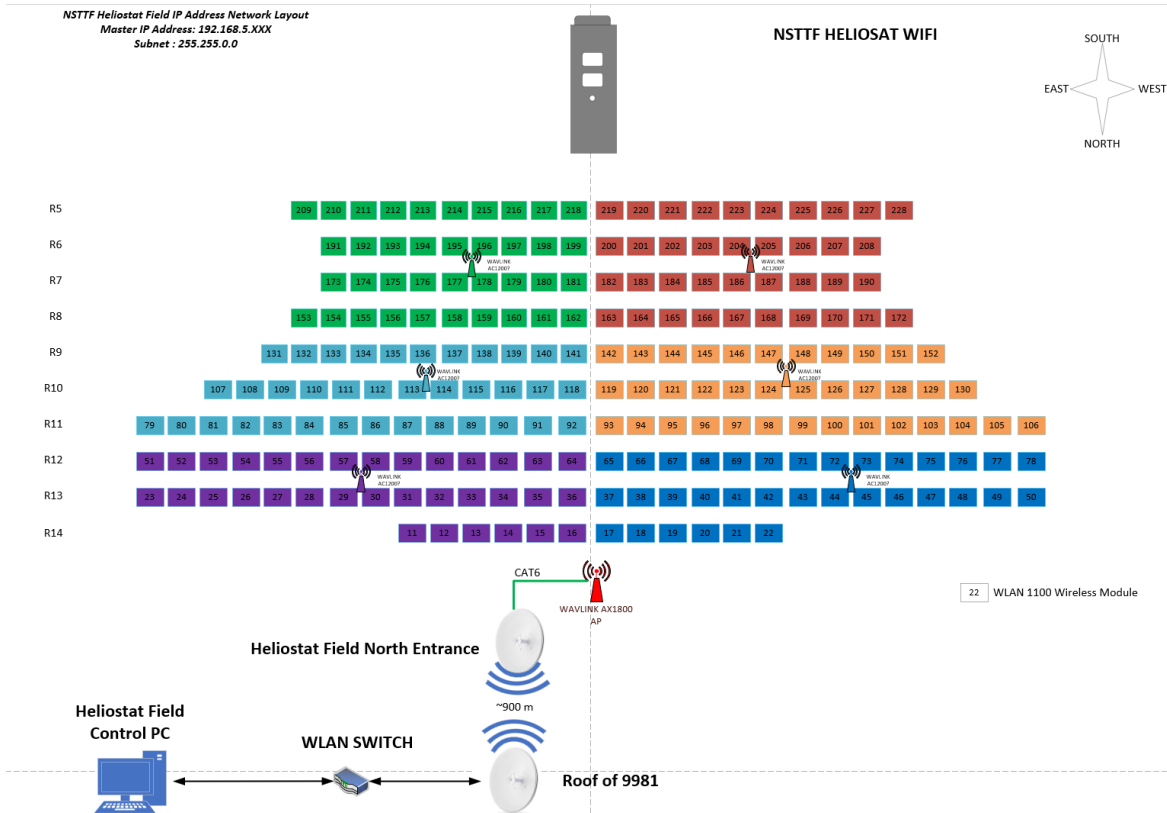
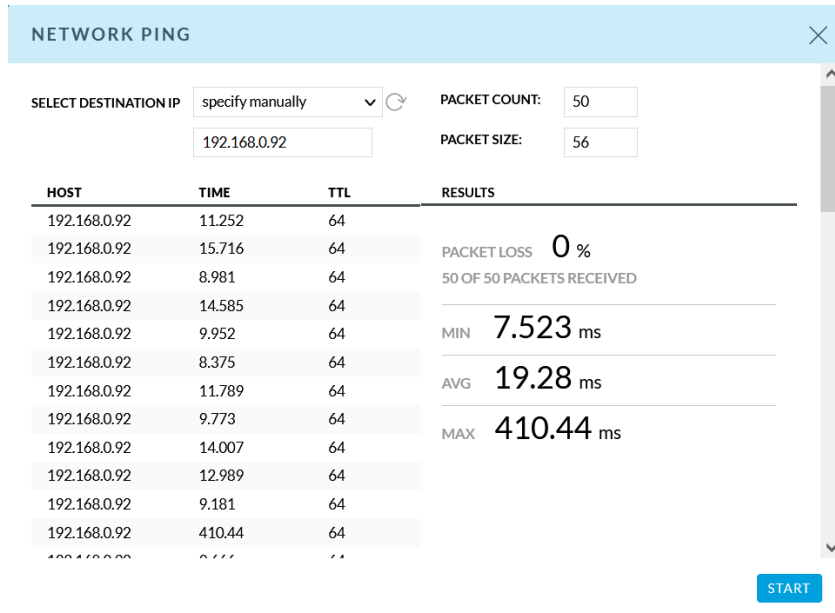
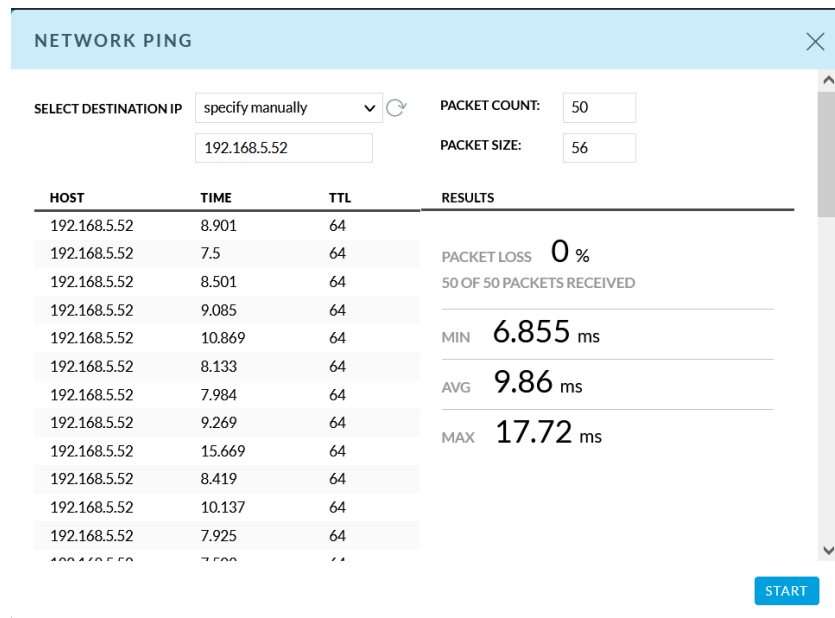


Figure 37. NSTTF Heliostat Field IP Address Network Layout.



**Figure 38.** Heliostat 12E02 Wireless Latency from Control Room.



**Figure 39.** Heliostat 12W10 Wireless Latency from Control Room.

In addition to Wi-Fi, the team also developed and integrated a mesh network capability for communications for the NSTTF heliostat field. This was facilitated as part of a DOE Helioclon Solar Dynamics, Request for Proposal (RFP) project. The team had originally been finalizing a heliostat package protocol and hardware, Figure 40 where testing of the hardware will be similar to that of the NSTTF WLAN.

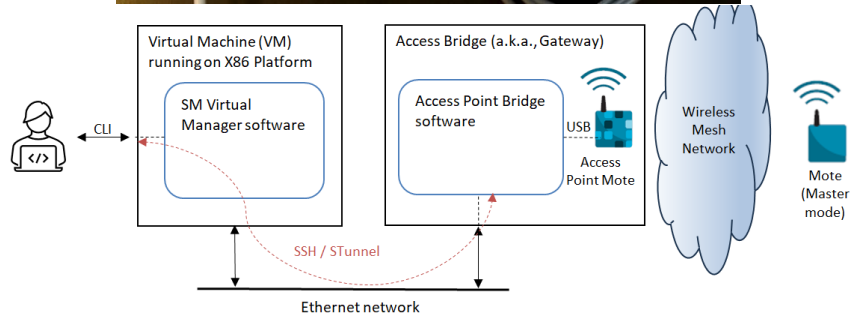
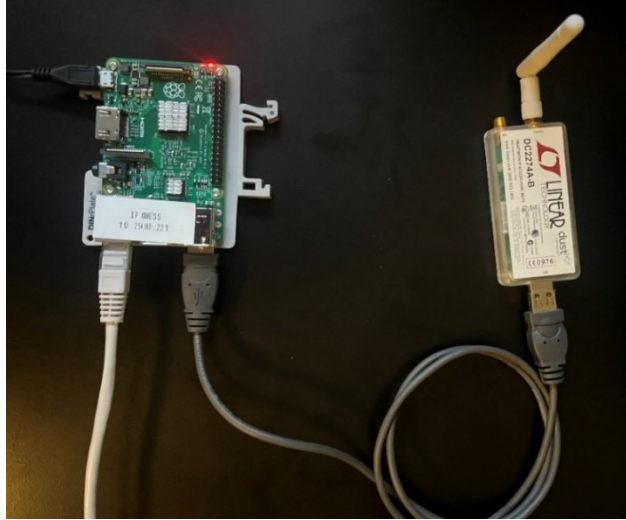


**Figure 40.** Mesh network hardware and design.

The Sandia team revised the Solar Dynamics RFP wireless protocol for the NSTTF heliostat field to allow confident communications. SNL and Solar Dynamics agreed on a final Heliostat Industrial SmartMESH Wireless protocol and FPGA interface (Figure 41) for implementation of the Smart Mesh grid technology. The Sandia team presented to Solar Dynamics the data structures of the data packages coming from each heliostat to be implemented within their setup more precisely to connect to the NSTTF heliostat field.

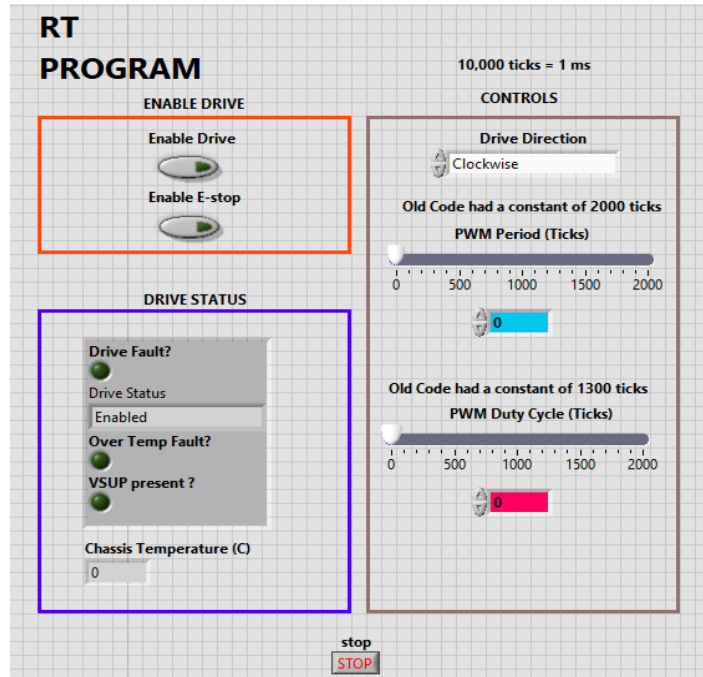


Figure 41. FPGA Interface User Interface

For the Industrial SmartMESH protocol each individual mote subsystem and their respective antennas and supporting subsystem (Figures 42-46) were able to be proven to communicate through a gateway antenna back to NSTIF Control Room. This integration has provided confidence to future CSP plant to allow Wireless Communication system to avoid any wire consumption and trenching. The results of this work has the potential to reduce the costs of field deployment significantly, by reducing the need of wired communications connections and extensive field deployment trenching and conduits.



Figure 42. Heliostat Mote Radio.



Figure 43. SmartMESH Gateway Antenna.

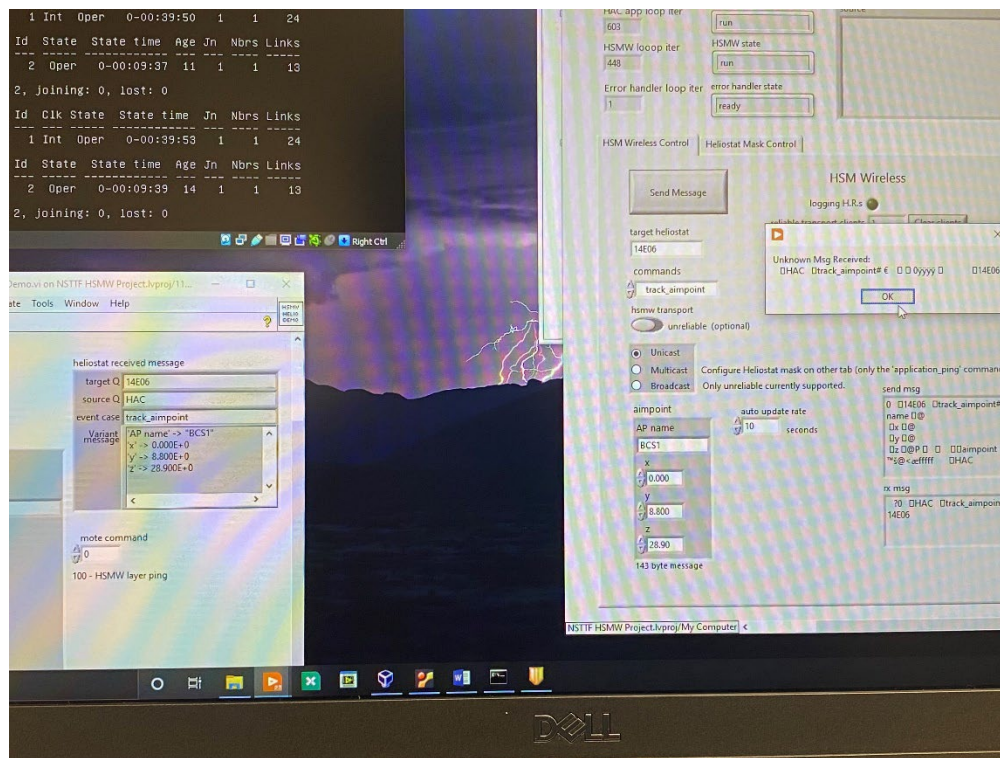


Figure 44. Full Wireless Integration with Radio Mote and VManager SmartMESH.



**Figure 45.** Gateway Antenna Installed at NSTTF 220 Level.



**Figure 46.** Embedded Planet Gateway.

The SNL team at the end of the project was able to demonstrate communications and operability with the Mote Radios connected and the AP gateway at 220ft level of the solar tower, where examples of the feedback for two of the Heliostats is shown in Figure 47: Heliostat ID 2 is 12E01 and Heliostat ID 3 is 05E03.

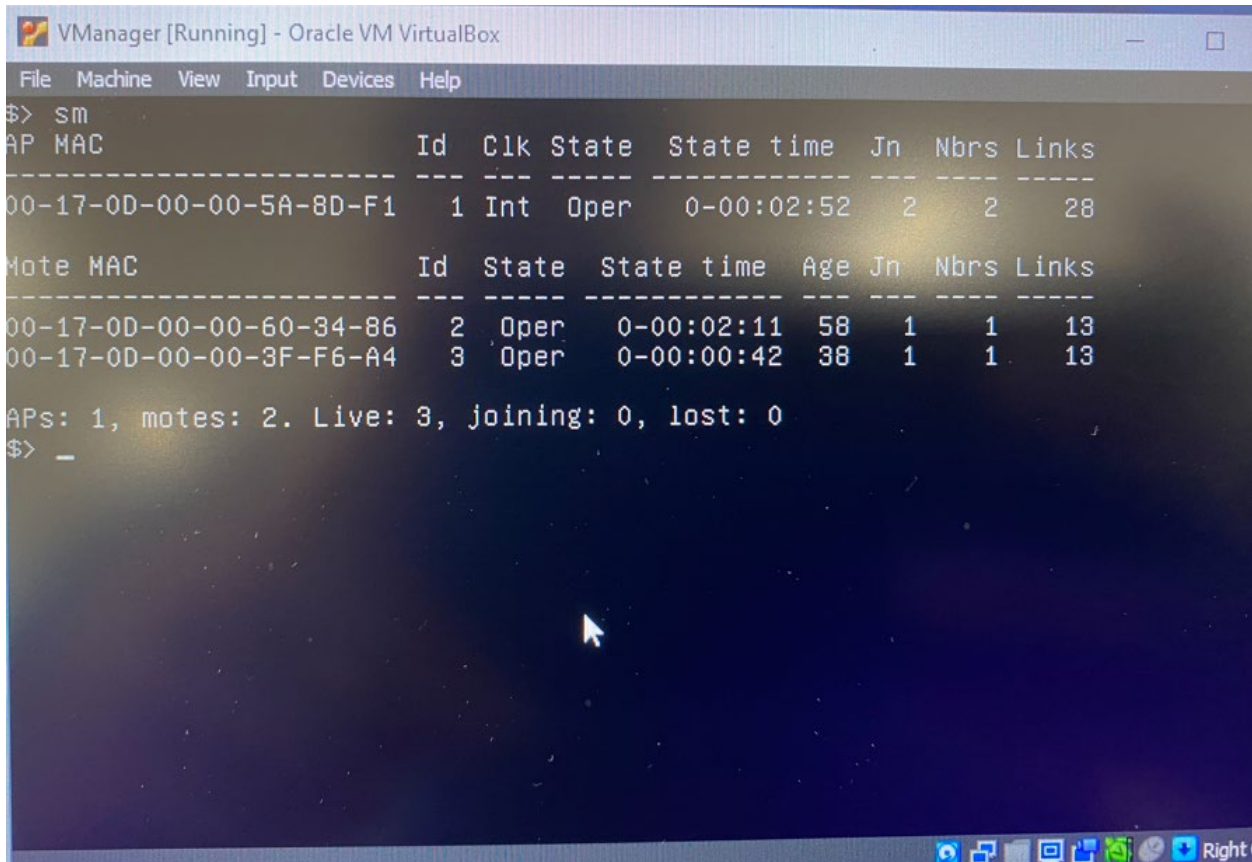


**Figure 47.** Two Mote Heliostats Mesh Network operability demonstration.

#### **4.1.4 Site Integrated NAS Data Historian**

To provide a more robust historical record of data pertaining to solar tower testing, as well as prognostics and health management (PHM) information, a Network Attached Storage (NAS) system was procured during Q2 to avoid any delays on supply chain shortages. With the NAS the technical team setup the operating system (OS) of the NAS with the correct RAID pools of the Hard Drives to store data.

The new NAS, shown in Figures 48 and 49 was also updated to parcel DOD data securely on a dedicated drive. The expanded storage for the DOE will allow for higher resolution data collection through both the multiple new sensors being integrated into the heliostat field as well as previously used sensors being carried over with this heliostat field refurbishment. These include the new GPS timer, DNI and GHI sensors, wind, and weather, the two DAQ's associated with the generation 2 tower, BCS camera, IR camera, and any modular sensor needed for DOE/customer projects. The team also has come up with solutions for how this system can have dedicated slots, or the development of a separate, dedicated NAS for more sensitive DOD tests.



**Figure 48.** Installed network attached storage (NAS).



**Figure 49.** Permanent Installation of NAS System.

#### **4.1.5 Hardware & Software Upgrades Small-Scale Test Beds**

Additionally, to de-risk the deployment of the new hardware/software upgrades, the team developed a controls and closed loop controls test bench which simulated a BCS target using a heat lamp behind a thin metal plate with motors driving the x-direction and y-direction. Sensors were installed to view the temperature profile of the metal plate. The closed loop controls software developed by Sandia adjusted the x-direction and y-direction of the lamp through the data collected by the sensors to center the lamp on the target. Figure 50 provides two computer aided design (CAD) drawings depicting the test bench.

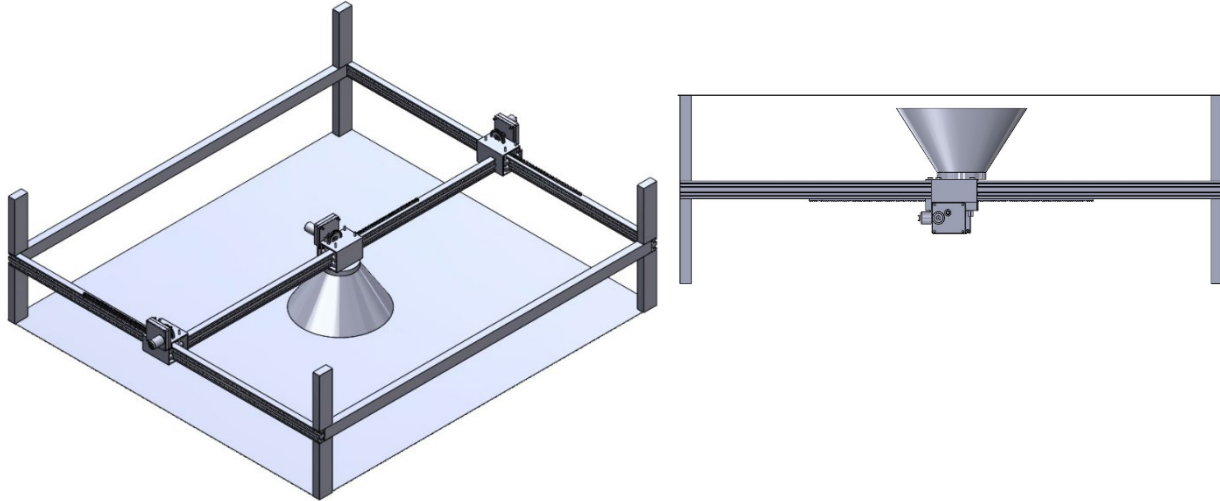


**Figure 50.** Small scale closed loop controls lamp test bed.

This testbed was developed to de-risk the deployment of heliostat movements with the upgraded field controls and communications, especially while the NSTTF heliostat field UPS was being refurbished during this project. This controls validation step and laboratory test bed was planned to be setup to assess controls architectures prior to deployment and validation testing of heliostats. The team was able to obtain all of the equipment to build a closed loop controls test bench, Figure 51. Experiments from this system was able to prove the controls for 16 heliostats prior to later stage testing.



**Figure 51.** Small-scale, single heliostat closed-loop controls lamp test bed.

#### **4.1.6 All-Sky Camera Cloud Tracking Capability**

During prior NSTTF field tests, the team ran into issues with cloud tracking, which impacted test

procedures while waiting for clouds to pass. Here, the team has also installed an All-Sky camera (Figure 52) within the NSTTF heliostat field control room to track clouds real time in a more efficient manner. This has allowed Test Directors and Heliostat Field Operators the opportunity to make more informed testing decisions such as with heliostat pointing and flux beam intensity timing.



**Figure 52.** NSTTF Control Room All-Sky Camera Output.

#### **4.1.7 Heliostat On-Board Power Development**

Additionally, the team also explored the employment of on-board power for the NSTTF heliostats since many commercial heliostat systems are currently using non-interconnected power to reduce overall heliostat field costs, such as with trenching and conduit runs. During this project the team was successful in setting up a PV panel and battery, and the ability to prove single motor operation for both azimuth and elevation, Figure 53. This setup consisted of a 24VDC 20A SLA Battery System, along with two 12VDC 20Amp SLA battery configured to produce 24VDC 20Amp system. The Heliostat had a Stand-by, which consumes between 250mA – 300 mA of current which is 6-7 Watts of power. When the Heliostat was running both motors 3.25A – 3.5A it consumed about 70-80 Watts of power. When moving just one motor is moving 1.4A – 1.75A it consumed about 35 – 45 Watts of power. Overall, the team is considering the purchase of two 12VDC LiFePO4 20AH Batteries and a Victron MPPT 75/15 Charge controller and put the system to work. A 245-Watt solar panel to connect to the charge controller is what was determined to ensure enough power margin for all systems to function well. The preliminary costs for purchasing a complete on-board system would be around \$700 USD.

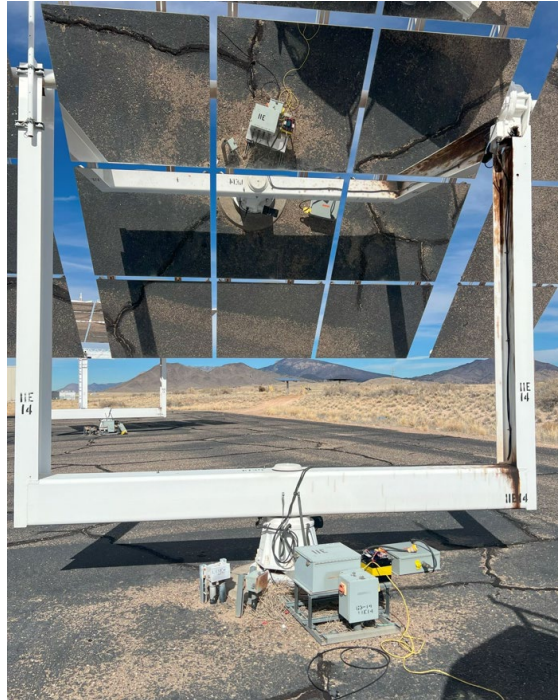


**Figure 53.** NSTTF heliostat on-board power setup and demonstration.

Demonstration for the on-board power system for a single NSTTF heliostat can be seen in Figure 54. The ability to provide power to each individual heliostat with a photovoltaic (PV) module and battery storage system also allows the field to have added resilience during power failures or during times when Mains power has disruptive harmonics.



Figure 54. On-Board Power Single Heliostat Development Setup.

#### 4.1.8 Field Upgrades Deployment and Commissioning

To demonstrate upgrade implementation within the SNL NSTTF heliostat field (Figure 55), the team first deployed 1 and then 16 heliostats, where implementation errors were assessed using the BCS panel at the 180' level of the solar tower and using other wireless and controls software checks within the NSTTF heliostat field control room. The heliostat controls were developed with respect to CRIOS and 16-bit SSI gray absolute encoders, which take in signals to move heliostats in azimuth and elevation.

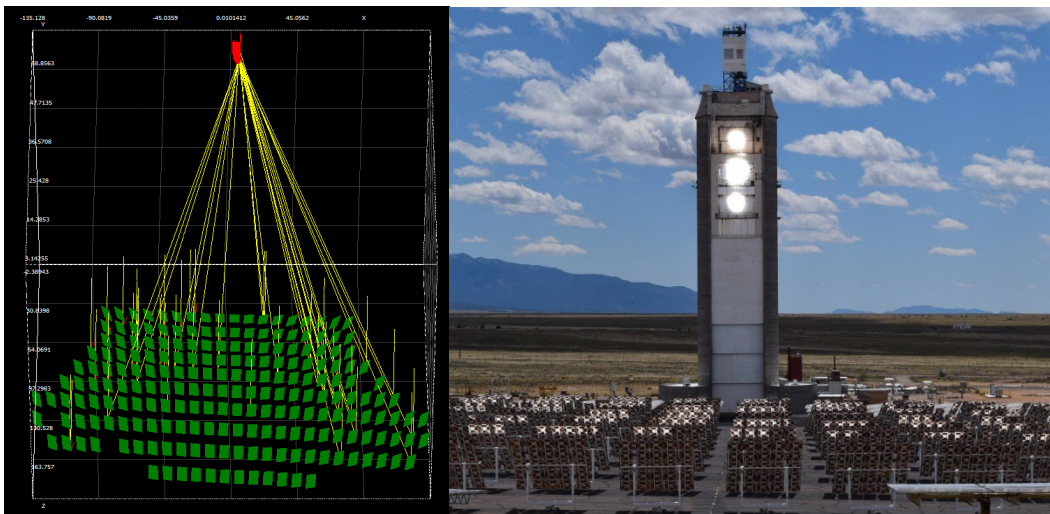
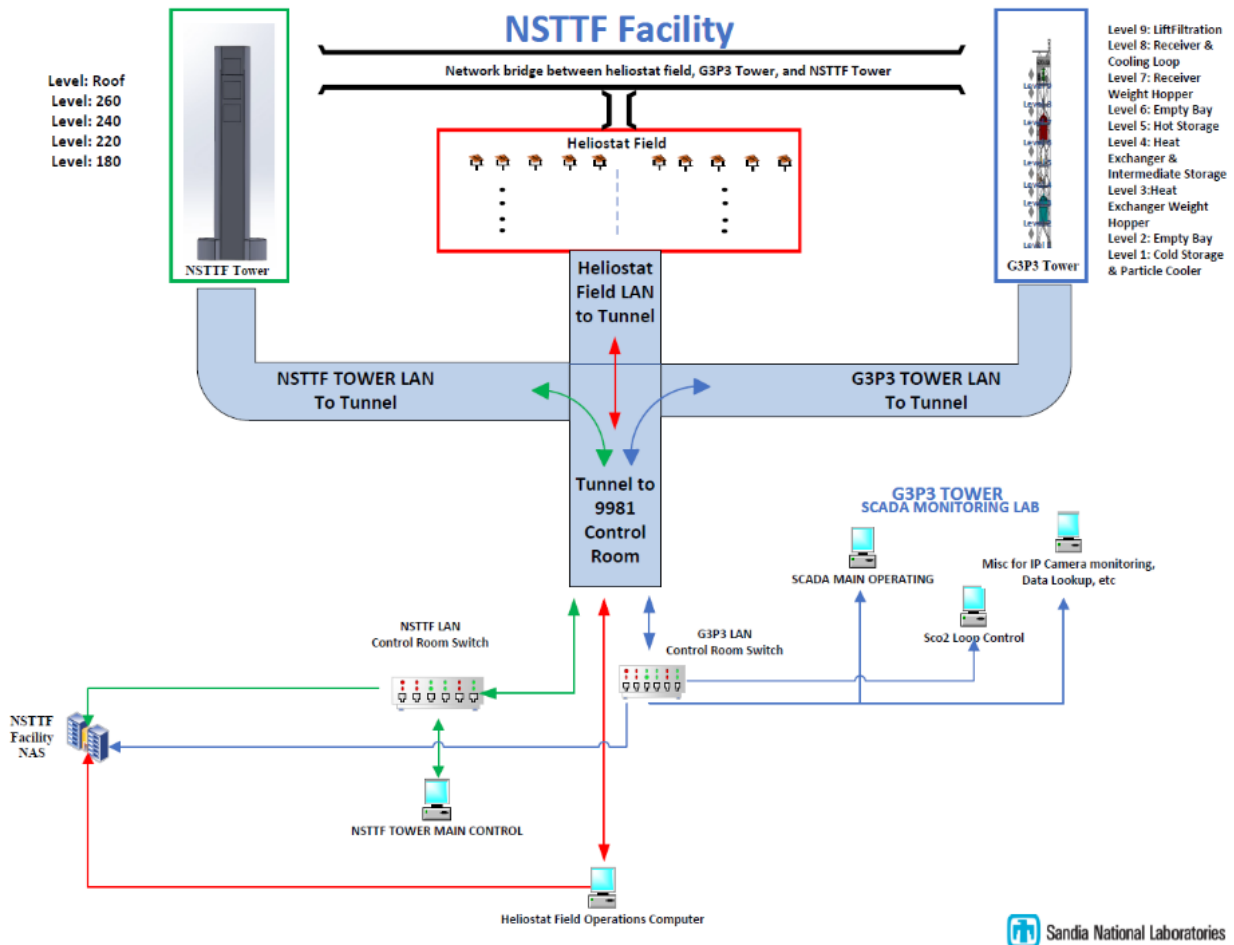


Figure 55. NSTTF Heliostat Field

The team also considered controls of the single heliostat field with respect to both the current solar tower and the new G3P3 solar tower, Figure 56. The system would allow the single distributed system controller (DSC) computer to move heliostats to either tower, though the team is currently investigating controls and inputs/outputs flexibility to ensure confident beam pointing.



**Figure 56.** NSTTF Heliostat Field Process Flow System

The process for the full field update to the new cRIO 9053 hardware, tied in with the newly built RT and Host codes was completed through multiple phases. Staging the deployment of the 9053 cRIOs into 218 heliostats needed to be accomplished without disruption of planned field tests for NSTTF customers.

Using heliostat 05W06, the initial tests replaced the old cRIO with the new cRIO 9053 hardware and proved the updated software could communicate with the new hardware correctly to control the heliostat. Tests included basic movements of both the azimuth and elevation motors as well as travelling to named target locations including “stow”, “face south”, and “line bottom”. A second test was performed using heliostat 12W05 to test the tracking capability of the reworked code using the new GPS timer system. Significant improvements in tracking were seen compared to the legacy code during this test: the heliostats no longer wobbled back and forth between azimuth and elevation angle gears when at the tracking location, but instead had continuous contact on the forward gear creating a smoother tracking spot and a higher degree of resolution. This improvement will show long lasting effects on the heliostat hardware as the gearing will not wear out as fast with the new configuration. After tracking continuously for 2 hours, the heliostat stayed within 0.02 degrees of the desired location. Figure 57 shows the refurbishment team completing the first in-field tests.



**Figure 57.** Initial Field-Testing Using Heliostat 05W06.

Additional testing was completed using a cluster of four heliostats to complete event testing as well as the same testing parameters listed above. New code was developed for event loading that minimizes heliostat operator user error. This update proved successful, with multiple events being loaded and tested over the course of the day. Extensive testing was initialized to show any anomalies when transitioning between event testing to tracking to manual control to SCRAM. During these tests, current draw for each heliostat was monitored and shown to be within acceptable ranges throughout the rigorous testing campaign. Figure 58 displays a schematic of the heliostat field with heliostats used in the initial testing shown in red, with Figure 59 showing the Tower after successfully loading an event file to individually bring four heliostats onto the tower and surround the BCS target.

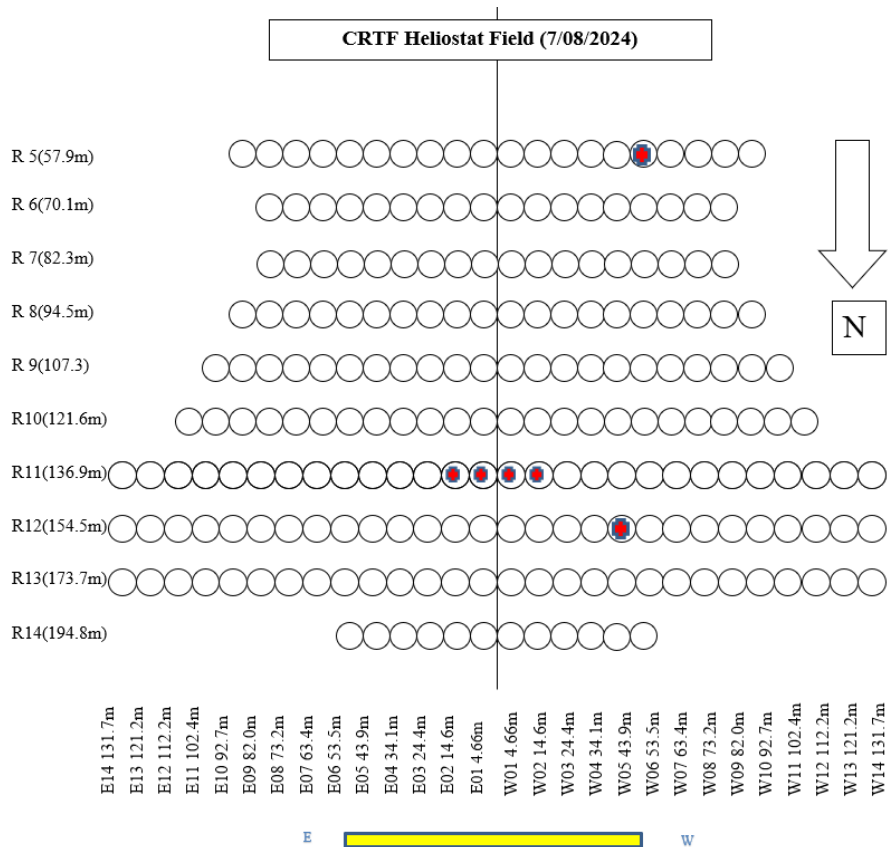


**Figure 58.** Heliostat Field with Heliostats Used in Testing Marked in Red.

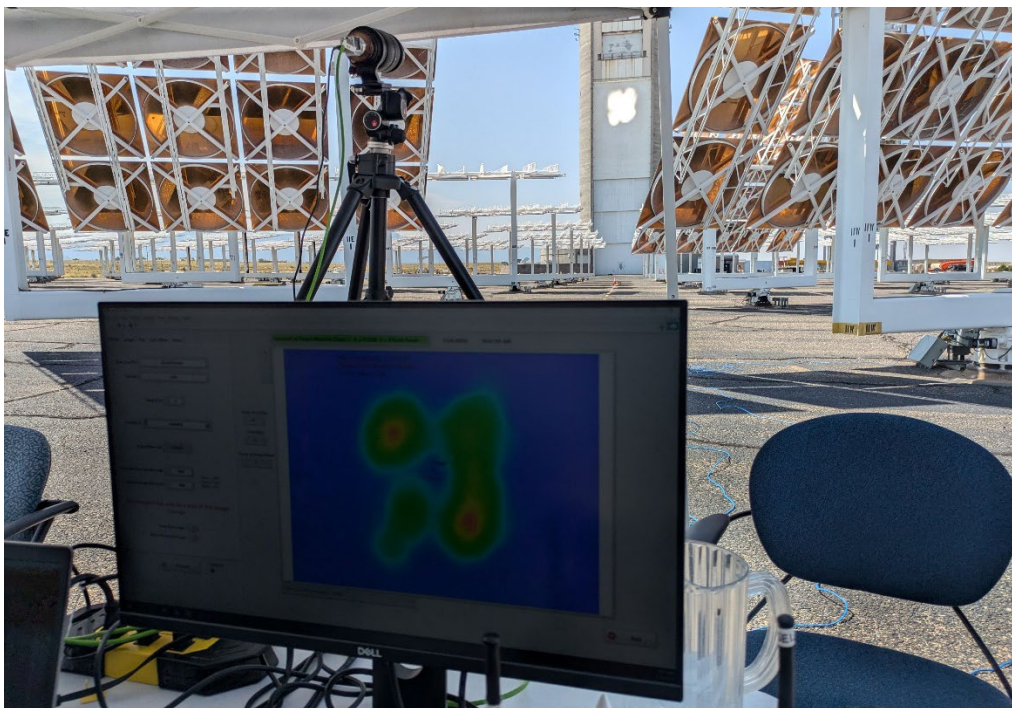


**Figure 59.** Event Testing Individually Bringing Four Heliostats onto Tower Surrounding the BCS Target.

The initial tests (using one heliostat, then four heliostats) were all accomplished from the field. Minor bugs were found in the new code during these tests requiring troubleshooting, then subsequent tests to confirm all prior issues had been resolved. Once confident in the full functionality of the code, the host was moved to the NSTTF Control Room and setup with the new primary graphical user interface (GUI), Figure 60 and Events software GUI, Figure 61.

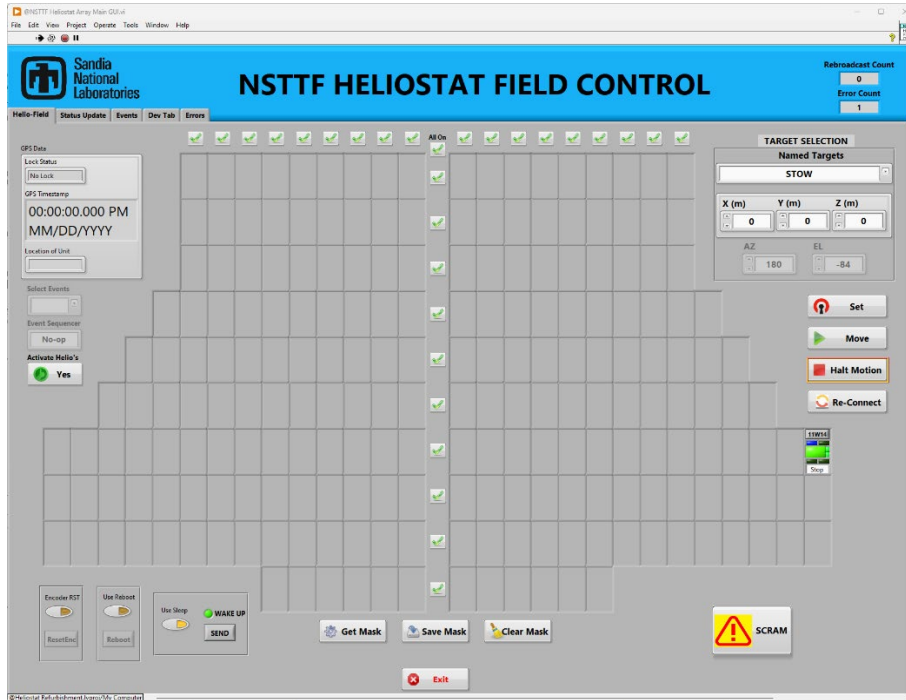


Figure 60. New GUI of the NSTTF Heliostat Field Array.

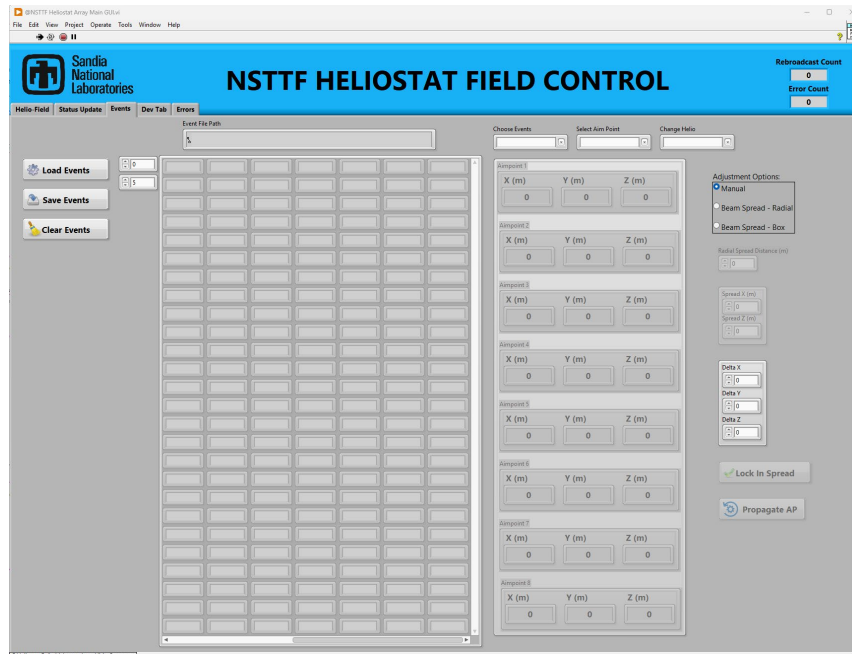


Figure 61. New GUI of Events Page.

Direct connection to 4 heliostats from in the field proved to be low impact to the site, with the team initially able to temporarily install the cRIO 9053 chassis on the day of testing. They then completed 8 hours of tests before returning the heliostats to the outdated system. These initial 4 heliostat tests focused on the functionality of the new FPGA code to confirm the correct movement of the heliostats with reference to the encoders. These tests also focused on the GPS timing of the system to validate the new firmware correctly read the time between the GPS timer, the firmware, and the RT to accurately point each heliostat to the requested target. After completing in-field testing, 25 heliostats were chosen to have the new hardware installed to verify the functionality of the Host and RT code from the NSTTF control tower. 16 of these heliostats were in a centralized block, with the remaining 9 being picked because they had shown recurrent issues under the old code (due to intermittency in communications or through increased amperage draw to drive worn motors) and the team wanted to complete rigorous testing using the new system on the heliostats that had proven to be the most problematic. The 25 block can be seen in Figure 62.

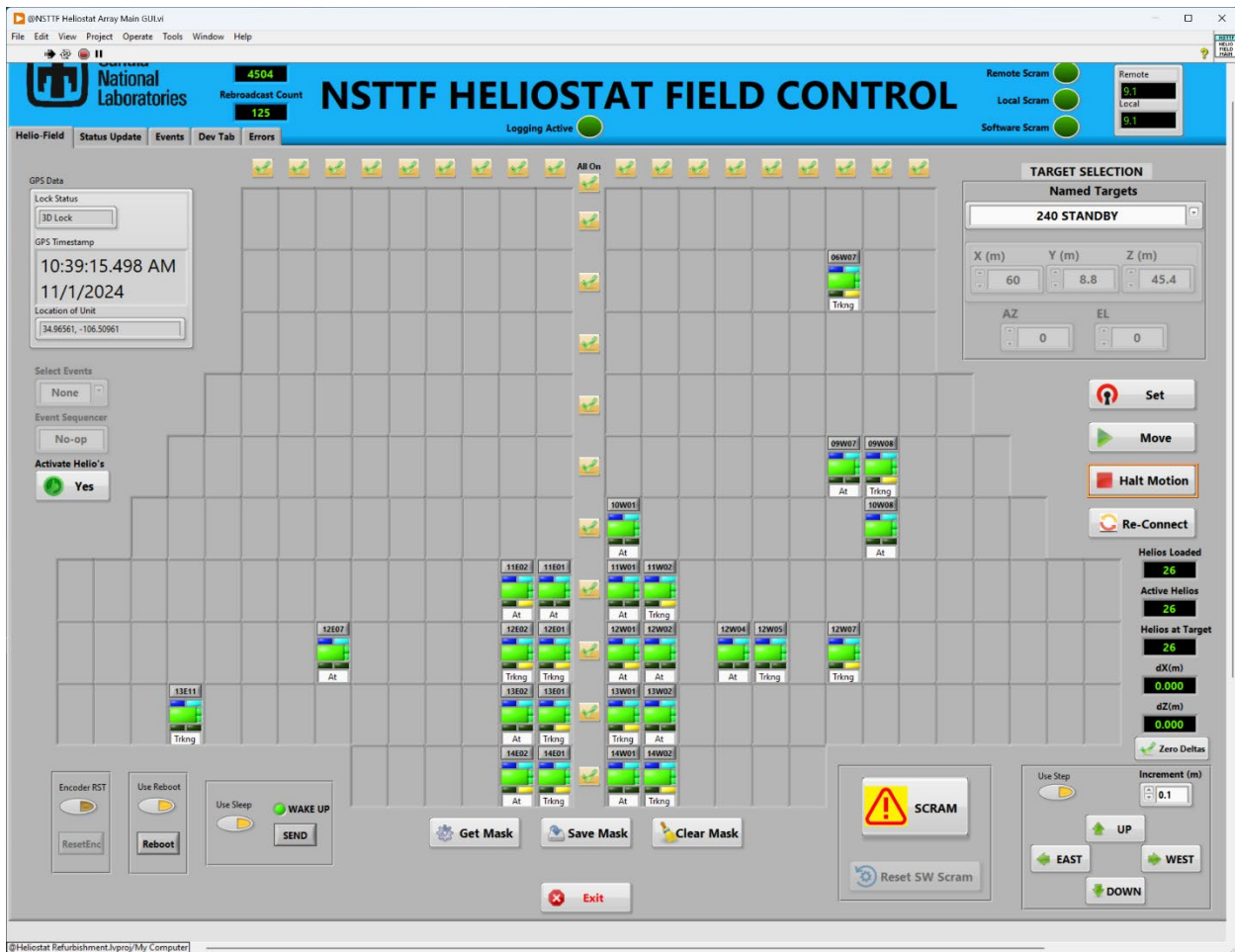


Figure 62. Initial 25 Heliostat Testing Block.

An additional central computer was installed in the control room specifically for the new cRIO testing. This allowed the team to switch between the new software and the legacy software still connected to the old cRIOs after each refurbishment test was completed. As the heliostat field was still actively acting as a test site for Sandia customers, following the refurbishment testing of the 25-heliostat block

with the new hardware and software, the old cRIOs had to be reinstalled in order to perform the required full field test campaigns by NSTTF partners.

Testing the 25-heliostat block allowed the NSTTF heliostat operators to move heliostats from the control room for the first time using the new software and hardware. While operating in a live scenario, the operators gave suggestions to the software developers on how to improve the GUI. Following a customer test which lead into a 5-week testing break on November 4<sup>th</sup>, the refurbishment team began the mass deployment and permanent installation of the new 218 cRIOs into the heliostat field. Over a four-day period, each heliostat control box was opened and cleaned, and the old cRIO was removed and stored (see Figure 63). The new cRIO 9053s had the driver modules installed and then were permanently installed in each control box before the control boxes were sealed.



**Figure 63.** Old cRIOs Removed and Stored.

SCRAM hardware was also tested by using the similar analog signal the NSTTF uses in the current SCRAM configuration. The new system has two incoming analog voltage signals at  $\sim 9.02$  Volts. One signal comes strictly via wire from the testing levels at the NSTTF Solar Tower. The other signal is located in the main control room where the HOST application is deployed, the SCRAM listens for the engagement of a push-down button that opens the  $\sim 9.02$  Volts signal that signifies a SCRAM has occurred. The team was able to test and validate the new SCRAM hardware with the actual heliostats and in different locations of the NSTTF Tower.

This page left blank

## 5. FULL FIELD DEPLOYMENT & COMMISSIONING

The final test campaigns focused on the optimization of the heliostat field and the timing issues that were realized during later test efforts when large groups of heliostats were activated. The GUI interface was updated frequently to meet the demands of the veteran heliostat operators and test directors (including the PI) to make the program as user friendly as possible without sacrificing safety and security measures. The team was able to overcome the challenge of only testing the field on Fridays, as the construction crews for the G3P3 tower were on-site Monday through Thursday. The team would use Monday through Thursday to do code writing and fix bugs found during the previous testing days, then preliminary tests of the updated code could be run at the “knocker”; located at 200’ level of the original tower, where the mock heliostat was installed and controlled through a cRIO 9053 with all of new software. This process proved invaluable with the limited field testing available.

After the multiple renditions and hours of testing, the final version of the heliostat GUI was deployed in mid-November 2024, as shown in Figure 64. Updates included each individual heliostat having indicators showing network connection status, sleep, and active notifications, tracking and moving statuses, and an “at position” status.

Additionally, the bottom right side of the GUI was dedicated to minute motion adjustments in the heliostats. Consistently, there was a desire to adjust heliostats by small increments, however that would require the operator to make time consuming changes to the three position locations. There would also be no easy way of returning to the original position. With the new GUI and software, these adjustments can now be made quickly and with the ability to track the changes made in 0.1-meter increments.

Above the incremental heliostat moves the figure shows the overall heliostat status. These three outputs display the number of heliostats activated, the heliostats currently moving, and the heliostats at position. This is immensely helpful when performing tests requiring a large number of heliostats. The operator can reference these outputs when in an off-target or standby position. When the heliostats are preparing to move from off-tower to a target, the desire is to have all heliostats converge on the target at the same time; this feature allows the operator a confirmation that all chosen heliostats have arrived at the preparatory standby position and are ready to go on target. This can be seen in 65, with 193 heliostats active and moving to the “BCS Standby” tracking location, with 180 heliostats having reached the position and 13 still moving toward the setpoint.

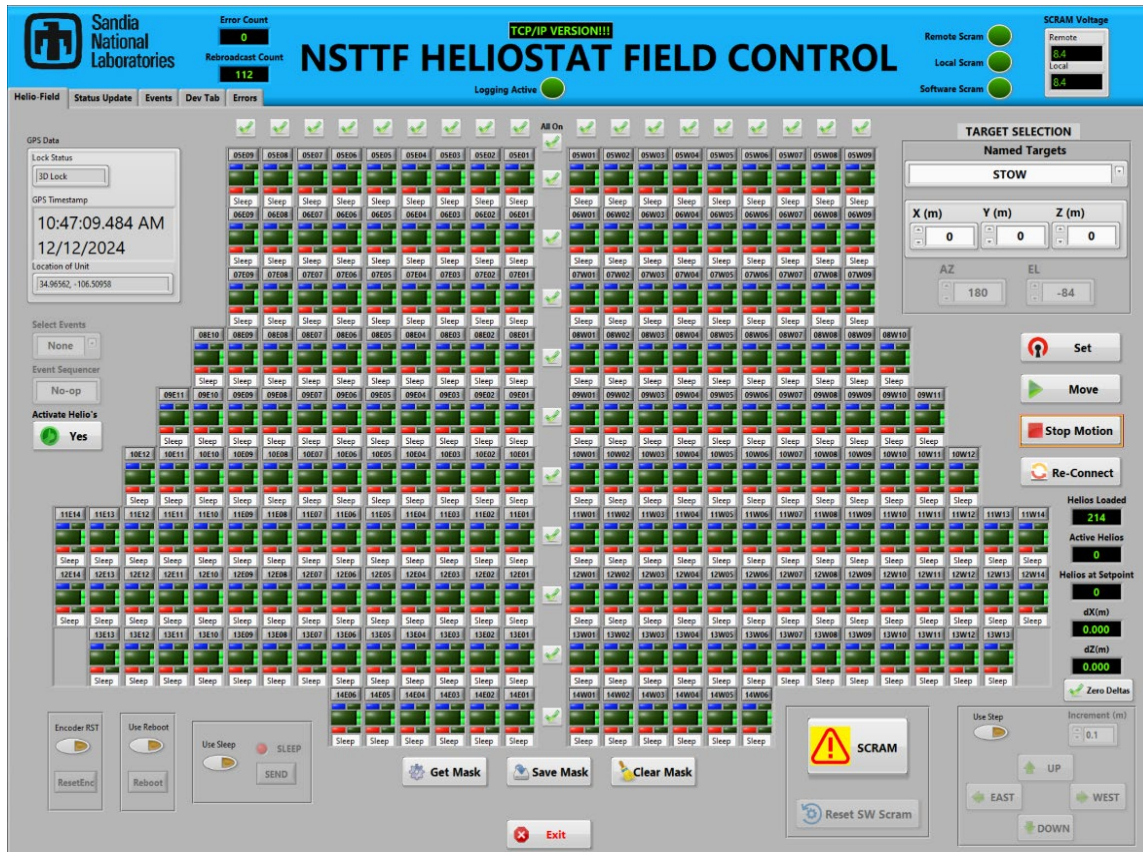


Figure 64. Final GUI.

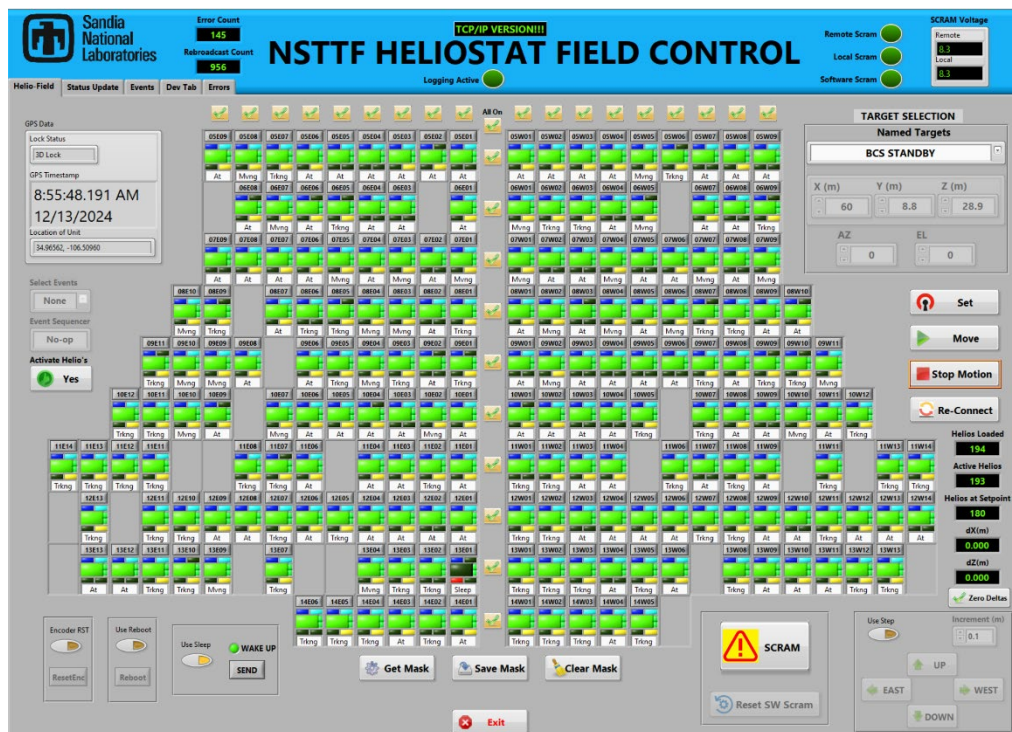


Figure 65. Active Heliostats moving to BCS Standby.

The GUI has also updated the visualization and functionality of SCRAM. The image seen in Figure 66 shows the full field in SCRAM. During SCRAM, the GUI still tracks the heliostat locations and displays the number of heliostats that have reached the SCRAM setpoint. All heliostat queues blink red and movement of heliostats from SCRAM cannot be done until SCRAM has been reset in the program in an effort to not allow an override of SCRAM. SCRAM was tested multiple times at all major tracking and target locations.

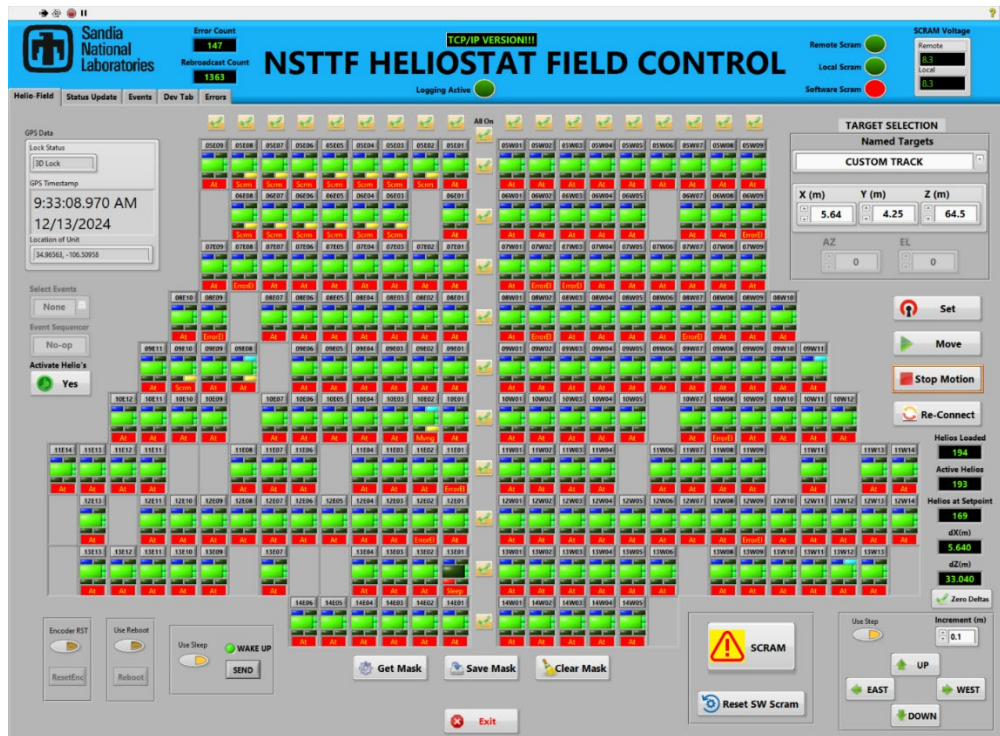


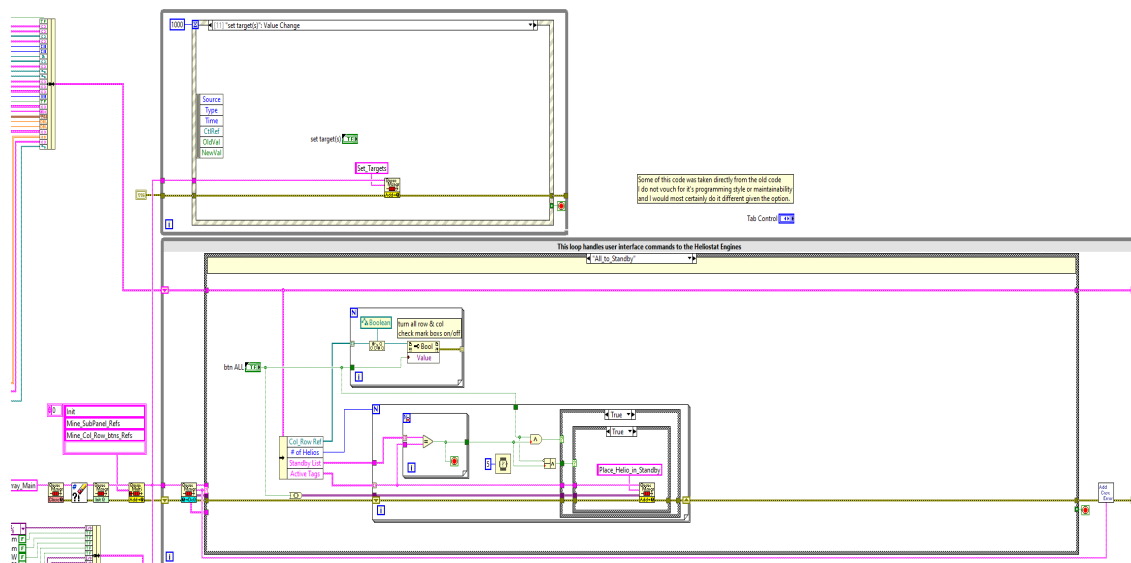
Figure 66. 193 Heliostats SCRAMING from the Tower Top Calibration Panel.

Figure 67 shows the heliostat field on the calibration panel for the first time with the new software. Prior to this test, all heliostats were set to track at BCS standby, then brought on individually to the BCS target to confirm the cRIO received the correct firmware and RT updates. Once all heliostats were checked for correct pointing, the heliostat field was taken to “line top”, then all heliostats were brought onto the calibration panel to collect flux data measurements and compare this data to flux measurements with the old code under the same heliostat numbers and DNI values to validate the full field flux levels using the new software.



**Figure 67.** Heliostat Field on Calibration Panel.

The ease of use for the Control Room GUI cannot be overstated. The updates allow for a more efficient running of the field, cutting down on potential user error when running tests, leading to higher testing confidence and lower stress levels when completing testing for customers. The new architecture software (Figure 68), and with the new GUI, troubleshooting specific heliostats is straightforward, with a dedicated tab (Figure 69) to see individual heliostat statuses and find if anything is abnormal in their operation. The event loader is also significantly easier to use, with the tab displayed in 70, the loading and executing of events takes minimal time and is easy to verify.



**Figure 68.** New LabVIEW Architecture.

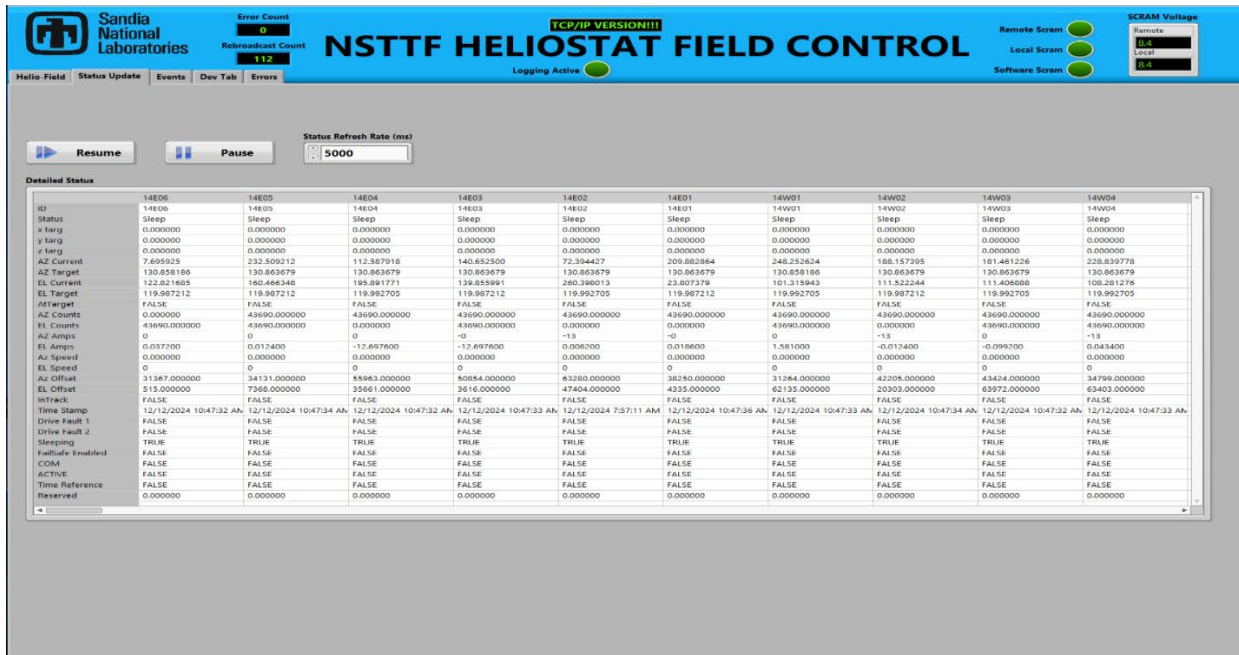


Figure 69. Status Update Tab.

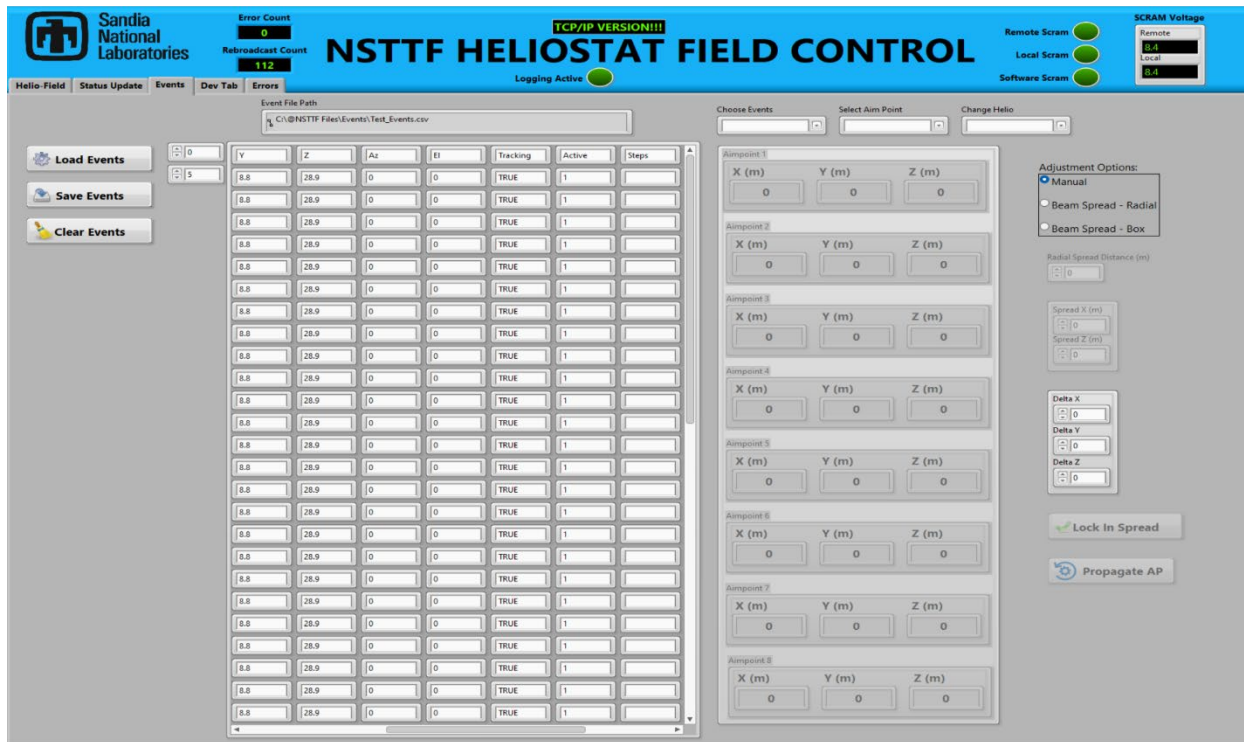


Figure 70. Events Tab.

Finally, at the end of the project, Two-Tower operations were assessed, however although the framework was completed, the implementation was not deployed due to the limitations of flux capacity of the Heliostat Field. With the framework built, the implementation into the RT should be easily deployable in the future and tested.

This page left blank

## 6. NSTTF CLOSED LOOP CONTROLS DEVELOPMENT

With the new development of the Heliostat Field Control software and upgrading the LabVIEW version. The team can now readily integrate Closed Loop Controls Algorithms to improve precise pointing, test new flux profile into receiver to achieve their steady thermal energy input. By using LabVIEW 2023 we can use the Python Node library to call python programs. This will allow Academia, Industry, and other interested parties to send Closed Loop Algorithms and here at the NSTTF can be integrated and tested. This may now provide the potential for a reliable operational certification from a Federal National Funded Laboratory for their equipment or subsystems.

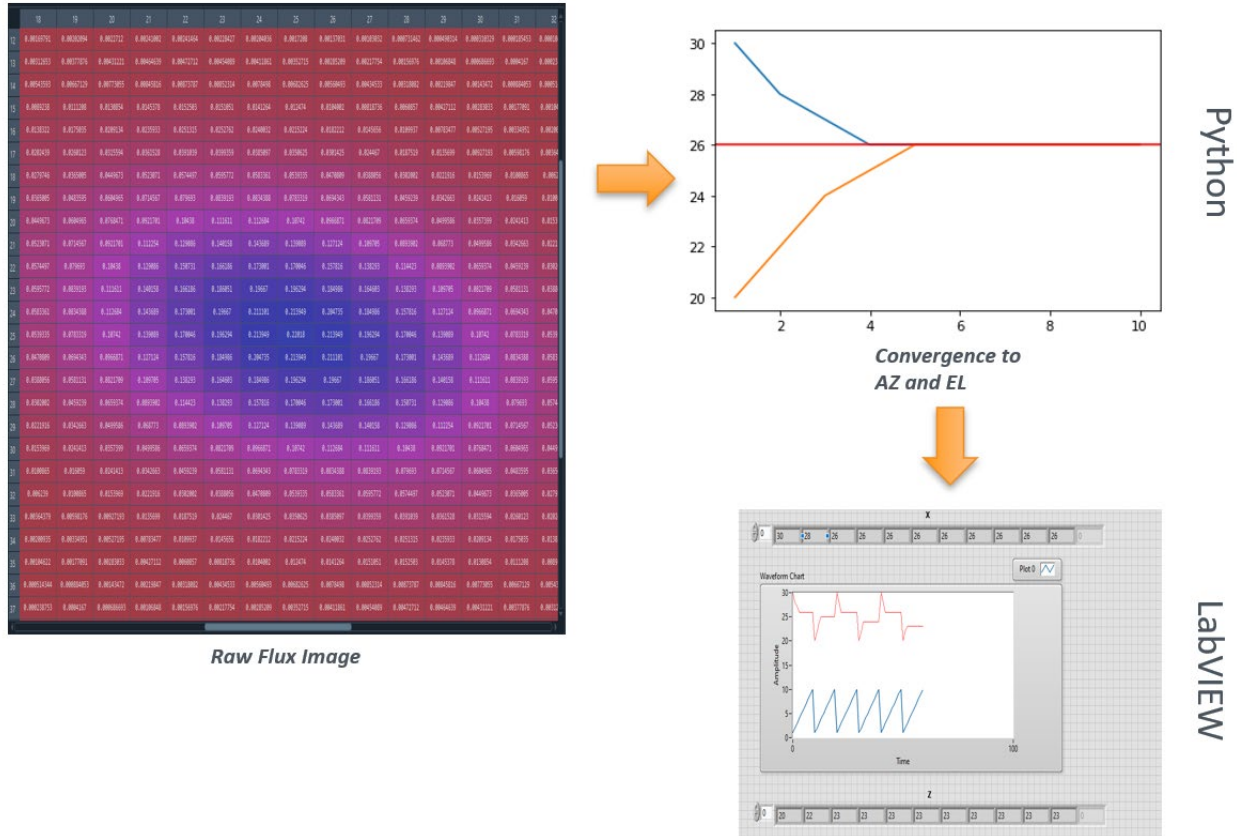


**Figure 71.** BLS algorithm to perform accurate Heliostat Pointing using Python and then Integrating it to LabVIEW to interact with Heliostat Hardware.

Additionally, during this project in conjunction with the DOE Heliocore program, the team also developed a baseline extremum seeking closed loop controls algorithm by which to test the overall software architecture and to be a nominal approach to serve as a reference to compare other commercial or R&D closed loop controls approaches. A particular extremum seeking algorithm that assesses the gradient of a BCS was developed to be this baseline approach. This closed-loop control algorithm uses batch least squares to calculate the gradient and calculate a new reference position for the system using power data from a BCS camera. When the system moves to the new reference position, the process starts again. The algorithm continues until it finds a position where the gradient is zero, which is at the peak of a unimodal distribution.

To test the algorithm, the small-scale test bed used to shakedown the overall upgraded controls system was utilized, again using three motors to move a BCS camera on two axes, a flashlight, and a

Laplacian target that hangs above the camera. The flashlight points at the Laplacian target and creates a distribution of intensity values that can be measured by the BCS camera. The setup can be seen in Figure 72, with external light sources extinguished to minimize interference with the initial data collection and calibration.



**Figure 72.** BLS Setup Under Dark Conditions.

The Closed Loop Controls Team also developed a LABVIEW code that takes an image, runs the algorithm, and moves the motors. The algorithm outputs a new pixel location which is used to tell the motors what direction to move and for how long. The motors move close to a constant velocity in pixels per second; using this and the new pixel location, it can be calculated how long the motors need to move. Figure 73 shows an image of the distribution, even though the distribution looks square, the algorithm can still be applied.

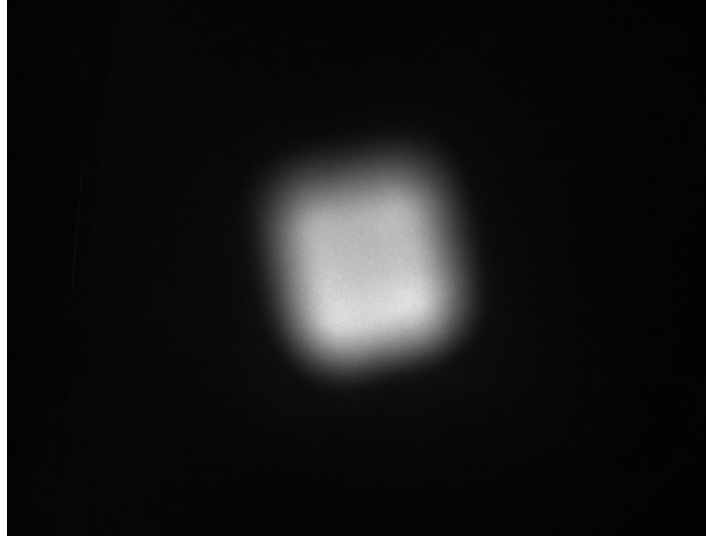


**Figure 73.** BCS IMAGE of flux source grayscale.

In order to optimize the performance of the code, the gain can be altered. The team utilized linear matrix inequality (LMI) and software-defined parameters (SDP) methods to find a gain that optimized performance. There are many gains that stabilize the system, meaning the peak value of the distribution is reached. However, the team is still working on a method to find a gain that stabilizes the system, is robust to varying distributions, and optimizes performance. Below are three simulations; the first two (Figures 74 and 75) having oblong distributions and the last one (Figure 76) having a more uniform distribution. For each simulation, the distribution and start position are randomized. In all the simulations, you can see that the system lags behind the reference positions, this is because the system takes time to reach each reference. Each simulation shows the system being stabilized and the peak power being reached.

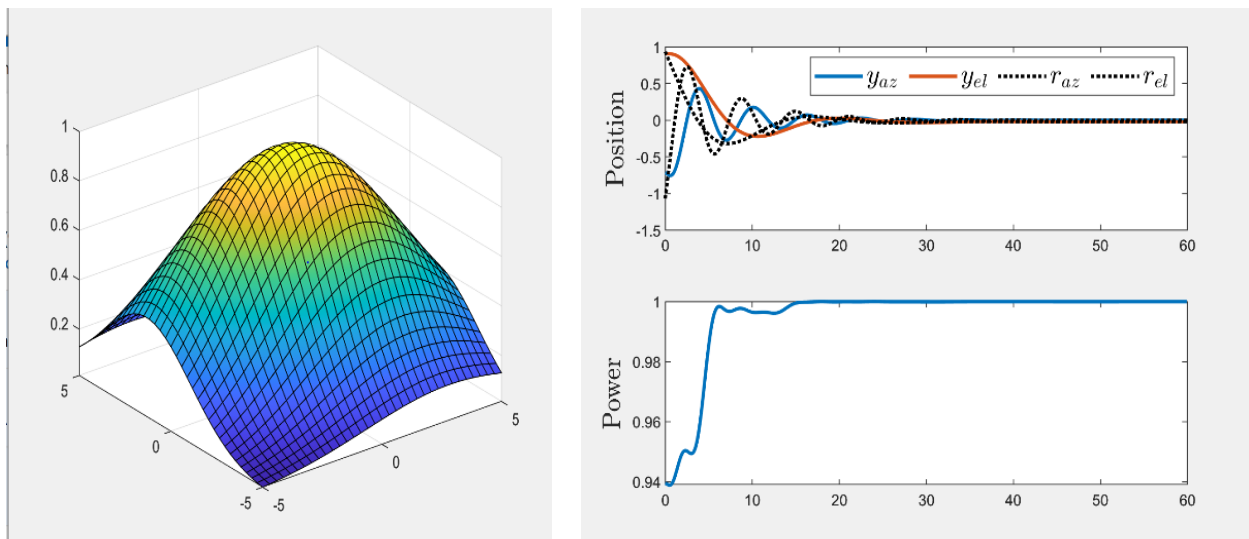


**Figure 74.** First BLS Output Finding Optimal Location.

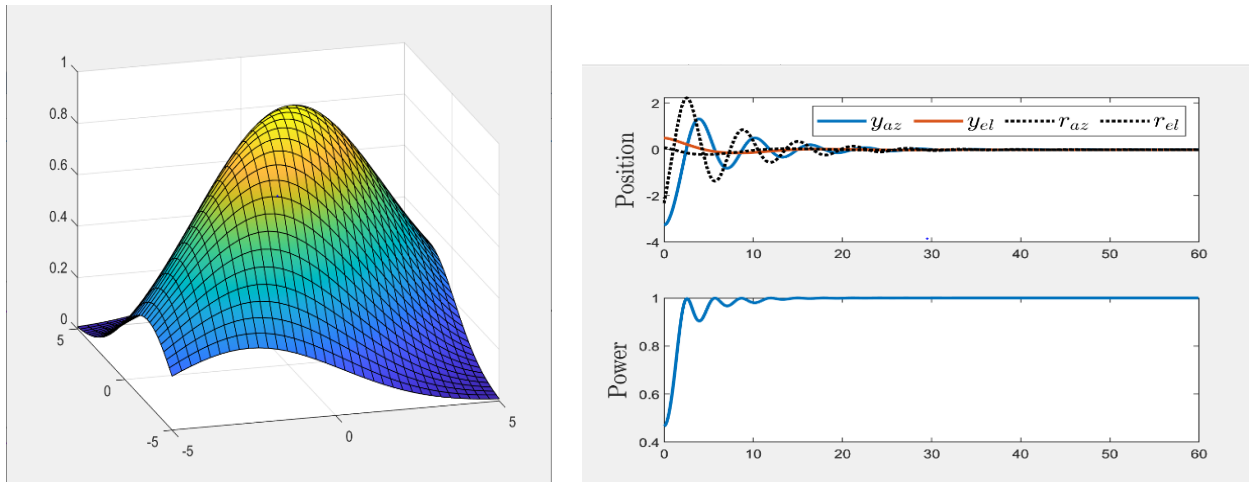


**Figure 75.** Second BLS Output Finding Optimal Location.

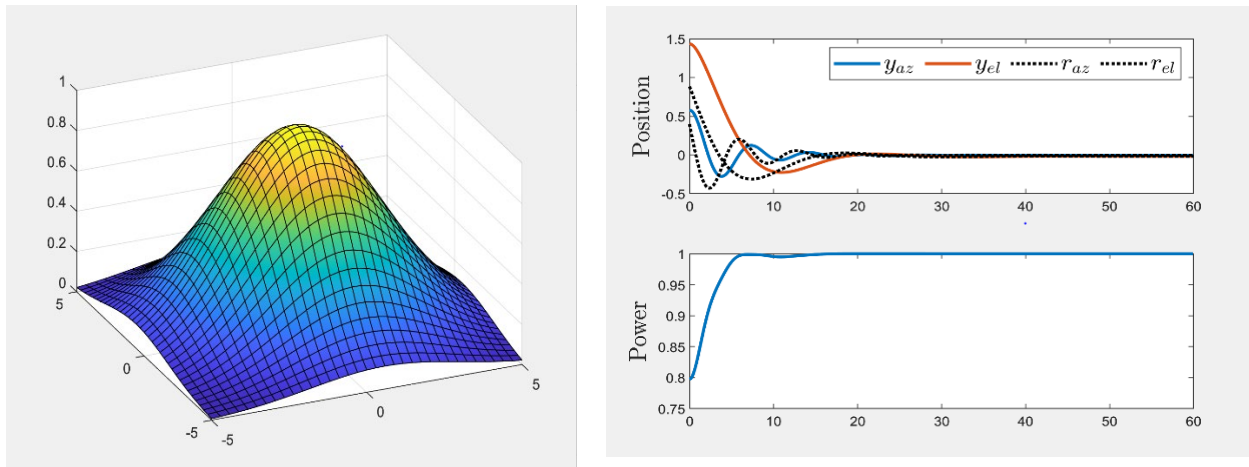


**Figure 76.** Third BLS Output Finding Optimal Location.

Using the setup in Figure 73 and this prescribed closed loop controls approach, the team applied the BLS function to the flux distribution in 19 to find the optimal location of the target. Using the Image data size in X and Y direction and dividing by 2 to compute the scaling factor of motion between each axis. The speed factor was also calculated to determine the amount of time each axis should move.

The movement figures are the pixel distance on the top graph compared to the Voltage steps on the bottom graphs in Figure 77 and 78. The system ID square figure is the square movement we did around the spot for the system ID. These movements were to perform system ID to create a state space model for stability analysis and optimal gain. Using a code that measures pixel weights to find the center of the light spot and calculating the pixel distance to the center pixel of the BCS camera gives the real time location of the motors in the X and Y plane. This location of the motors is then used to calculate the motors respective velocity in the x and y direction. These velocities were found to be about 15.5 Pixels/Second. The team then used this value with the Real time optimization algorithm to find the distance in pixels that were needed to move (Figure 79). Then dividing this distance to find the amount of time the motors would need to run to move that distance.

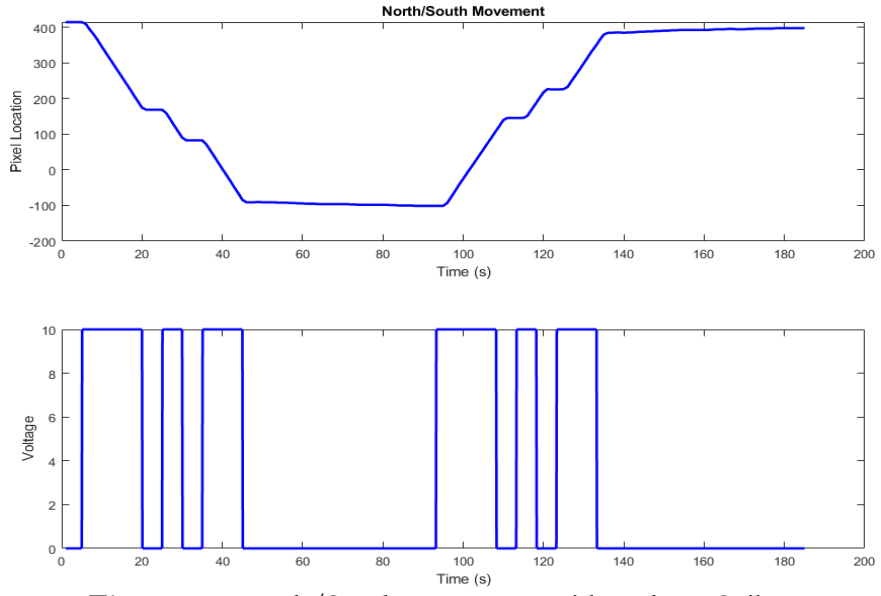


**Figure 77.** North/South Movement with Voltage Spikes.

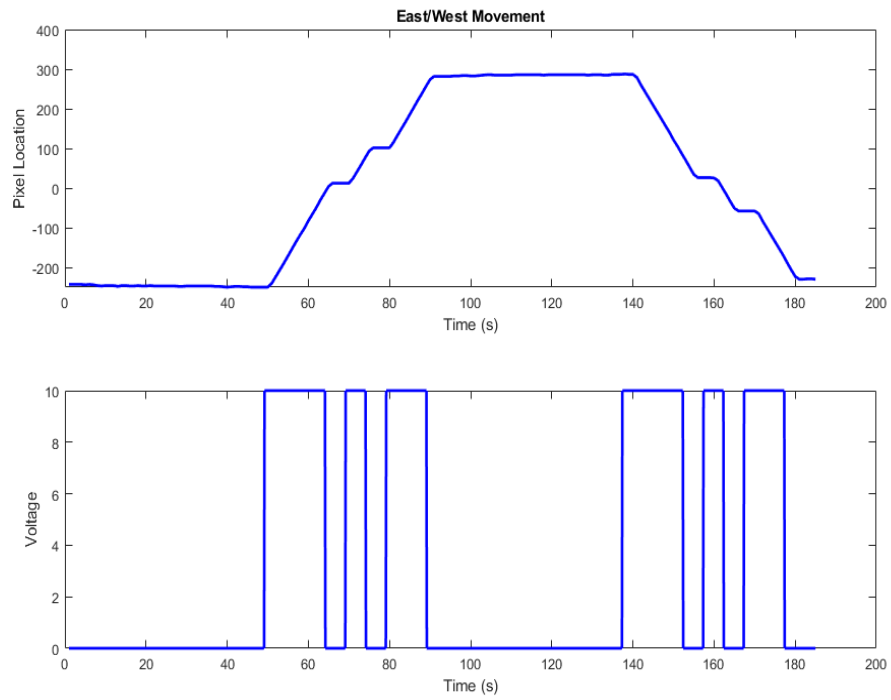


**Figure 78.** East/West Movement with Voltage Spikes.

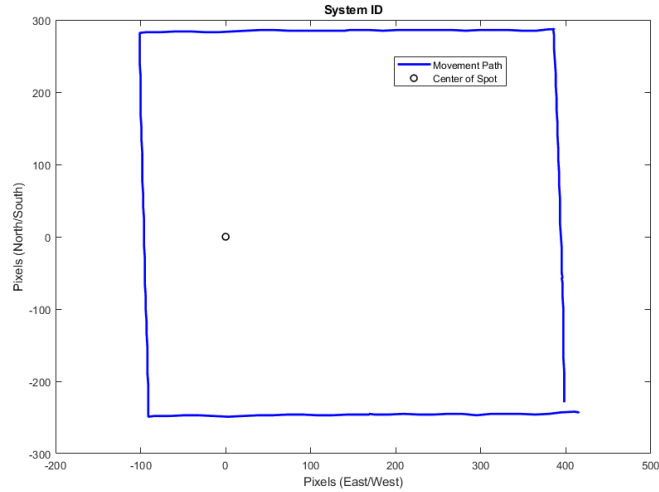


**Figure 79.** System ID Environment of the BLS Scale Size.

From the closed loop controls validation tests ran on single, 16 and full field heliostats, the results ranged from 85% of max power to 95% of max power. During the test, the closed loop controls, real-time optimization (RTO) algorithm was applied for 10 iterations. Ideally, the algorithm would be operated continuously throughout the day. Figure 80 shows the comparison of the maximum pixel value of the entire image against the value at the reference pixel. Additionally, Figures 81 and 82 show the BCS change before and after the RTO was applied. The algorithm achieved 95% of the maximum power on the tenth iteration using the extremum seeking closed loop controls algorithm. This test shows that the RTO algorithm does move the sunspot to the reference location by showing the increase in power at the reference pixel from almost 0% power and climbed to 95% power. Therefore, the ability to deploy and realize closed loop controls within the upgraded NSTTF heliostat field was demonstrated.

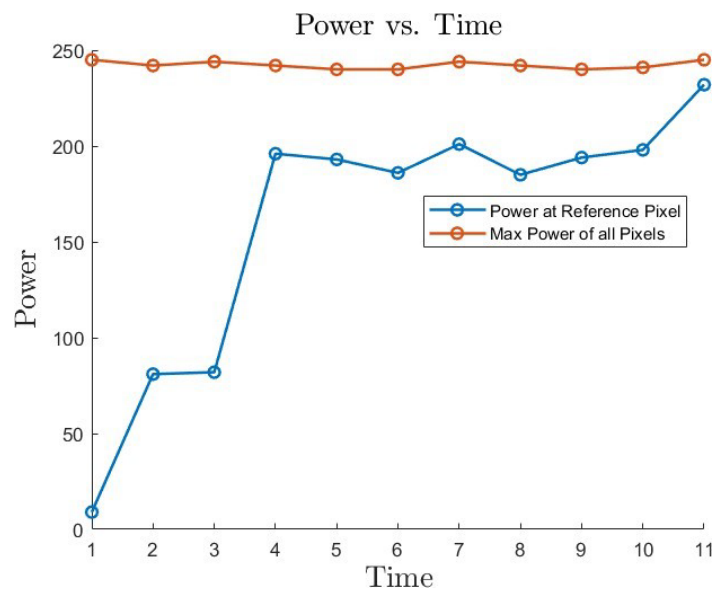


**Figure 80.** Power vs. Time. This figure is a comparison between the max pixel value and the value at the reference pixel using the closed loop control algorithm.

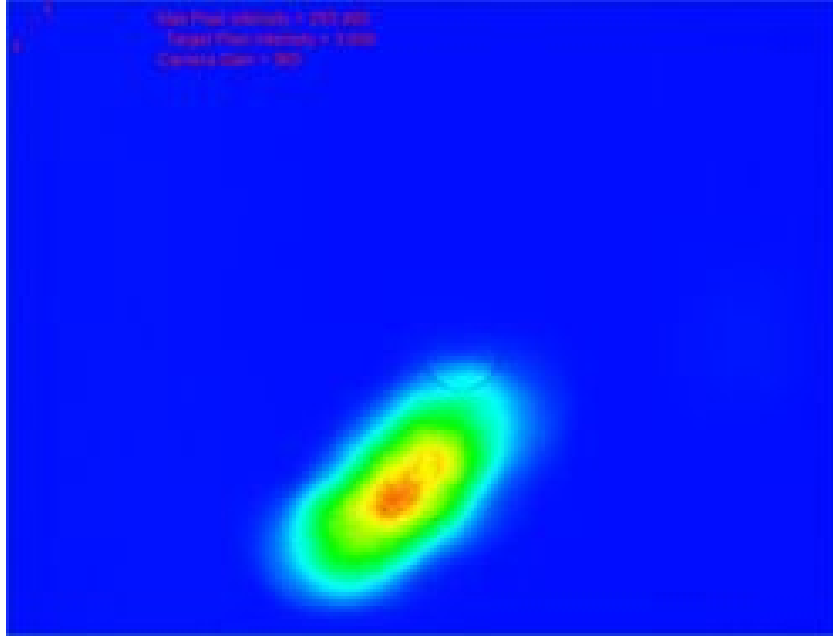


**Figure 81.** Actual Heliostat Image. This figure shows the heliostat alignment before using the RTO algorithm.

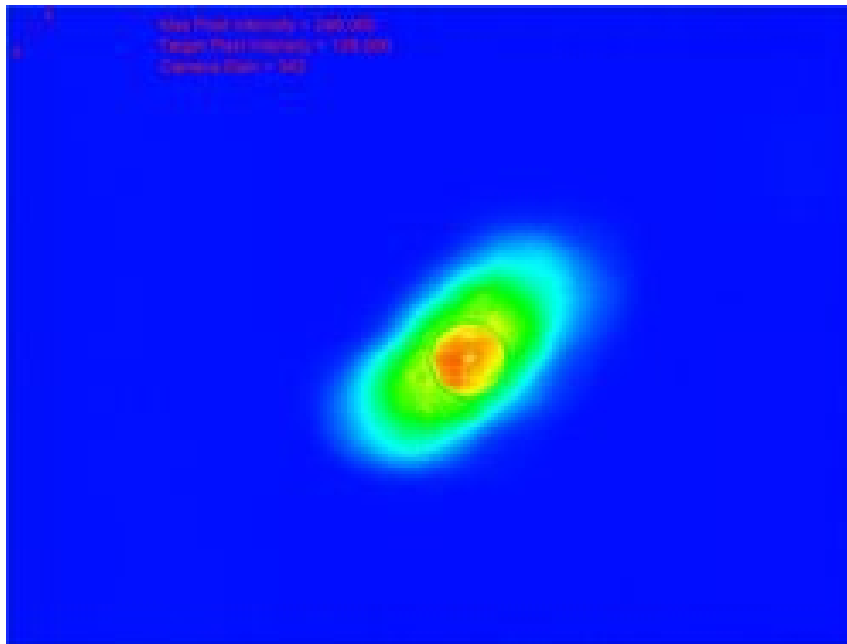


**Figure 82.** Actual Heliostat Image. This figure shows the heliostat alignment after using the RTO algorithm.

## 7. OVERALL NSTTF HELIOSTAT REFURBISHMENT EFFORT IMPROVEMENTS

As described earlier, the Beam Characterization System (BCS) at Sandia National Laboratories monitors the beam quality of the NSTTF Heliostats [2]. This system adjusts the central focused shape of the Heliostats into a desired [X Y Z] location and performs a flux measurement to obtain solar flux across a uniform distribution of the heliostat beam. The old heliostat field control software showed a large error drift and miss pointing from the nominal target. Figure 83 shows the nominal BCS image vs Figure 84 show the amount of adjustment into the nominal location.



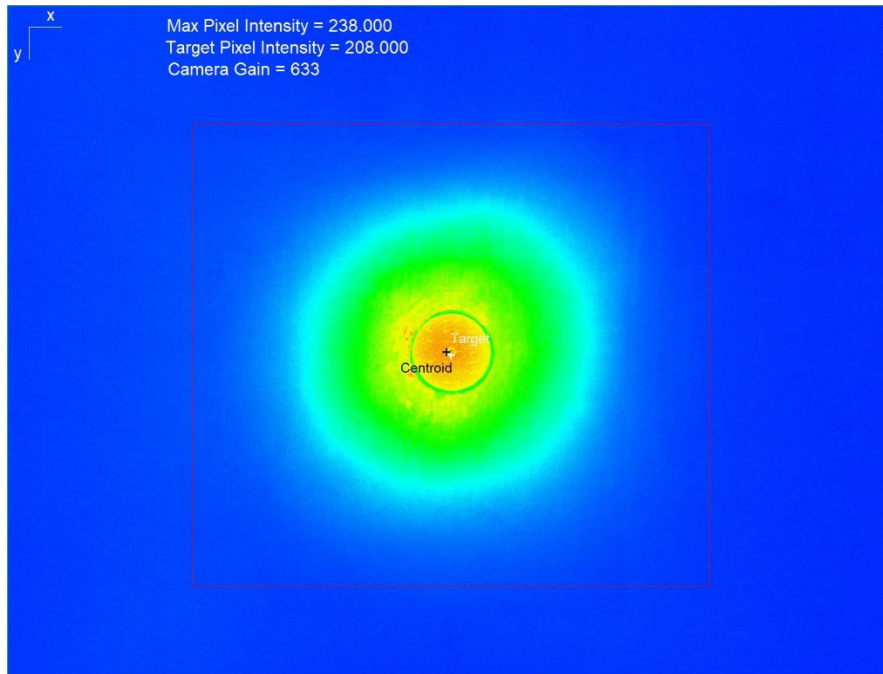
**Figure 83.** Nominal Location.



**Figure 84.** After Adjustment.

Although the adjustment is relatively minor, this correction can affect the flux level by 10-20 W/cm<sup>2</sup> with a range of 50-100 Heliostats in use. With the new Heliostat Field Control Software, the BCS

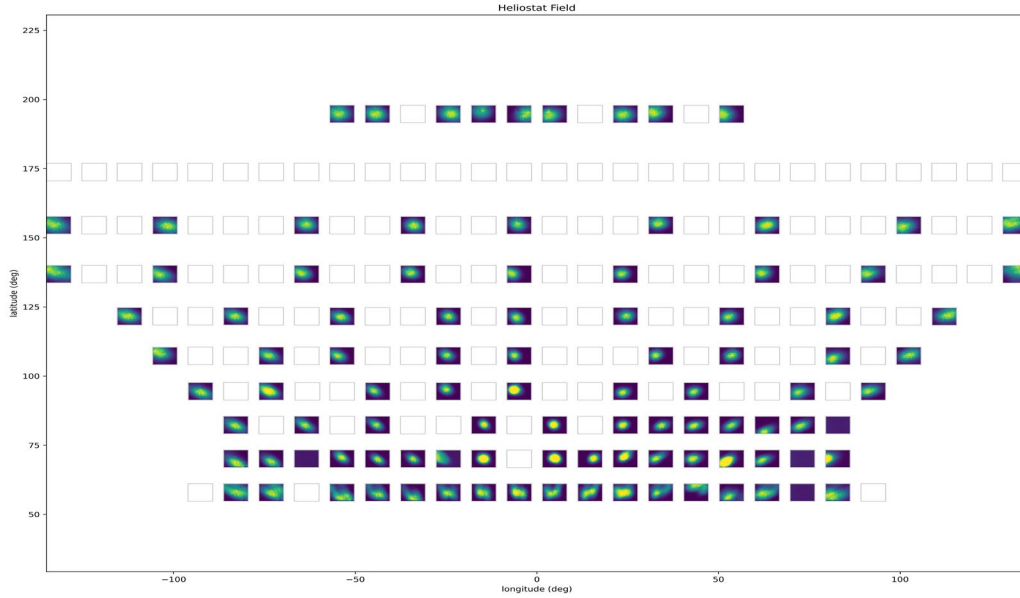
shows a major improvement to pointing by showing a correct nominal location, presented in Figure 85.



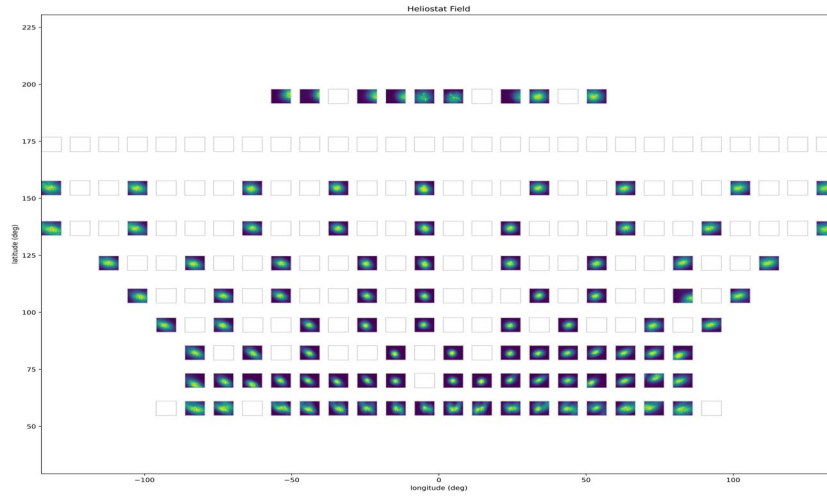
**Figure 85.** Shows nominal pointing with new Heliostat Field Control Software, no adjustments.

## 7.1 Flux Improvement by Heliostat Field BCS Scanning Techniques

During testing the team noticed implemented the controls developed during this project, however the team noticed initially that flux measurements were not corresponding to the theoretical ray tracing of SolTRACE models, causing uncertainty among NSTTF customers. To improve the flux measurement without disrupting the optical properties of the Heliostat, the NSTTF team created a scanning motion profile for 100 Heliostats using the new heliostat field control software to create over 100 scans per day – computing these scans in a post process measurement of  $\Delta X$  and  $\Delta Z$  to improve pointing and subsequently showing flux improvement by putting the uniform flux distribution across the flux gage measurement device as accurately as possible. Figure [4] show the BCS images of a set of these scans, with Figure 87 showing the BCS images scans after adjusting the X and Z location of the pointing of the heliostats. Both comparisons show a more central pointing after adjustments toward the flux gage distribution.

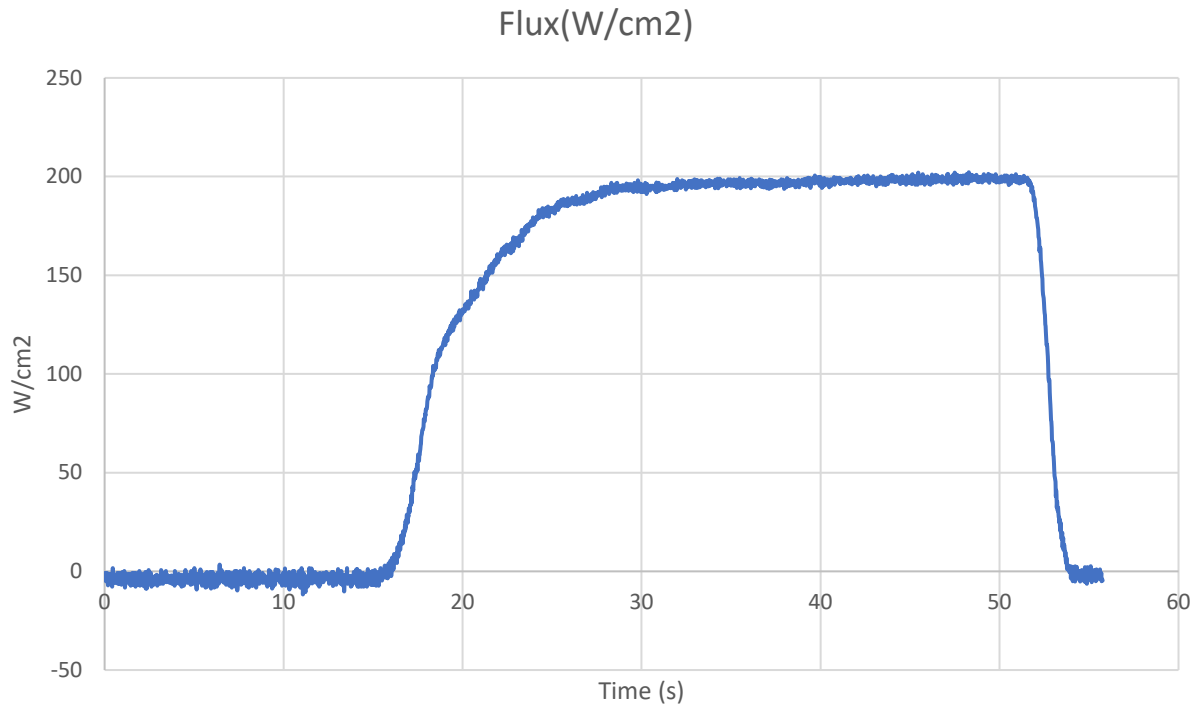


**Figure 86.** Before Corrections.

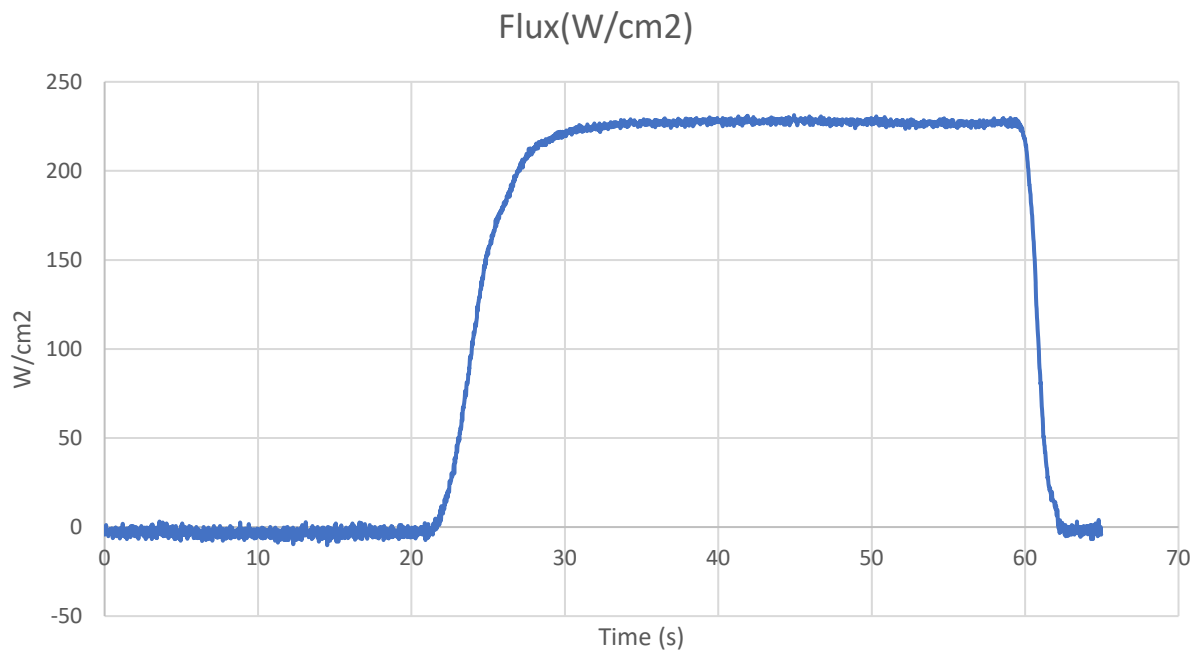


**Figure 87.** After Corrections.

Flux measurements were taken with original aimpoints XZ and process XZ measurements to show the improvement of the overall flux measurement. Additional scanning needs to be performed to complete the entire 214 Heliostats and achieve flux levels of  $> 250 \text{ W/Cm}^2$  during periods when the direct normal irradiation is  $980 \text{ W/m}^2$ . Figure 88 shows a premeasurement of flux without scanning the 100-heliostat group, with Figure 89 showing a post measurement of flux after scanning the 100 heliostats.



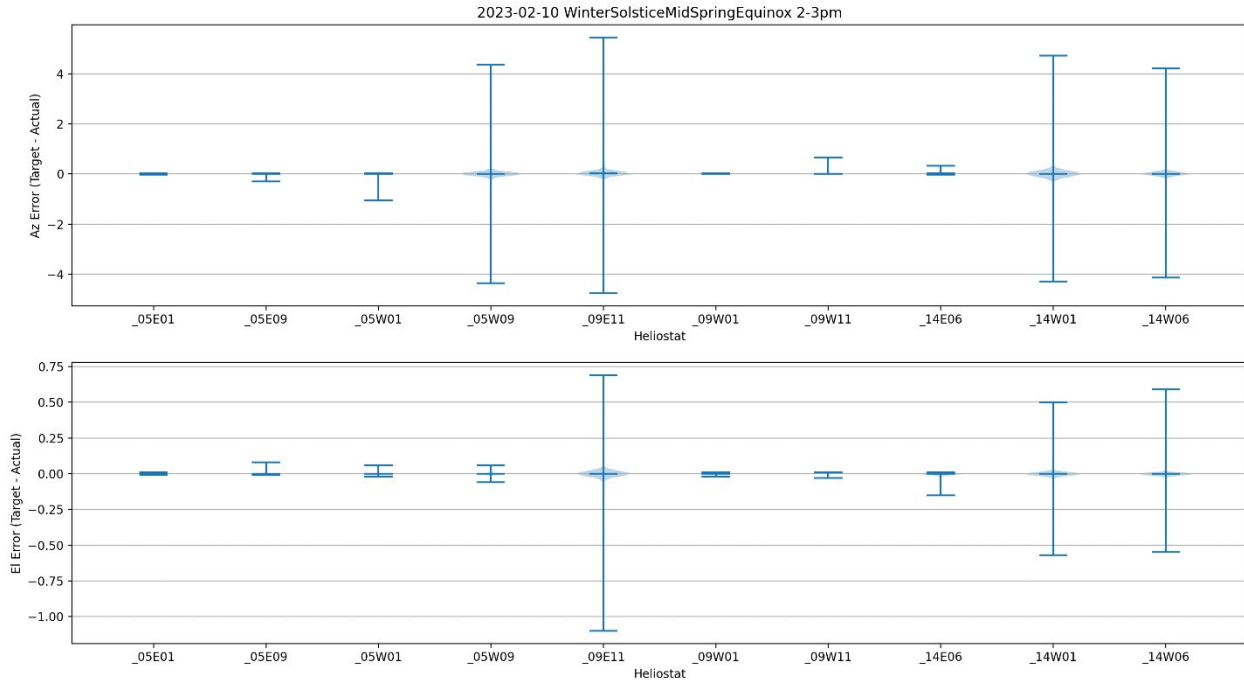
**Figure 88.** Flux measurement pre scan.



**Figure 89.** Flux measurement post scan.

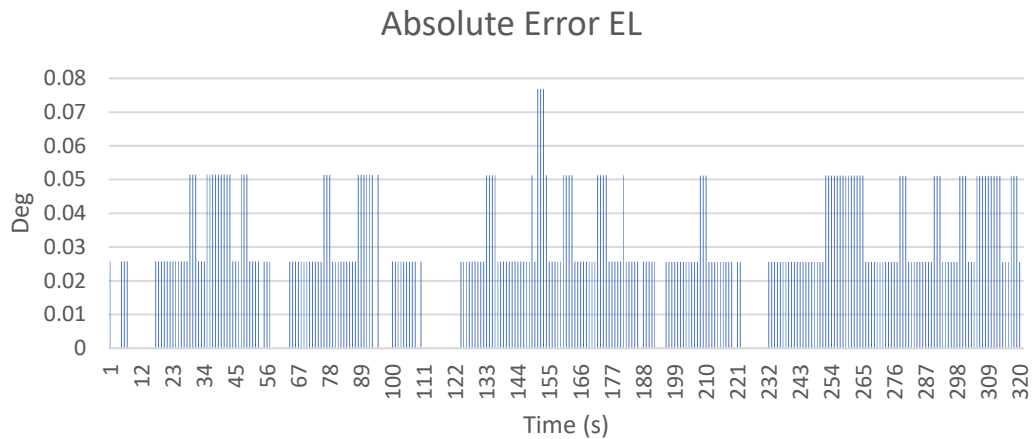
## 7.2 Tracking Performance Improvements

The new software architecture has shown slight tracking performance improvement compared to the old control software. Figure 90 shows the old tracking data of a set of heliostats.



**Figure 90.** Old tracking error calculation of old software.

Old and new heliostat data sets were compared showing an improvement of tracking for azimuth axis  $< 0.025$  deg (0.43 mrad) and for elevation axis  $< 0.09$  deg (1.57 mrad), shown in Figures 91 and 92 respectively.



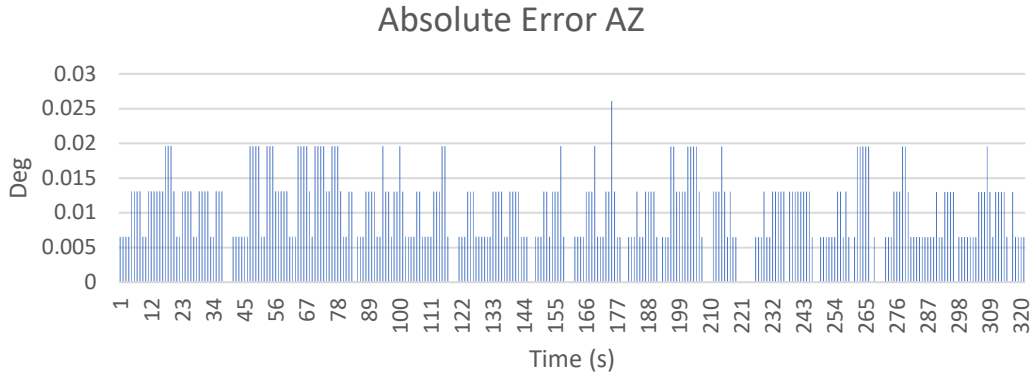


**Figure 91.** Az and El tracking error calculation of old software.

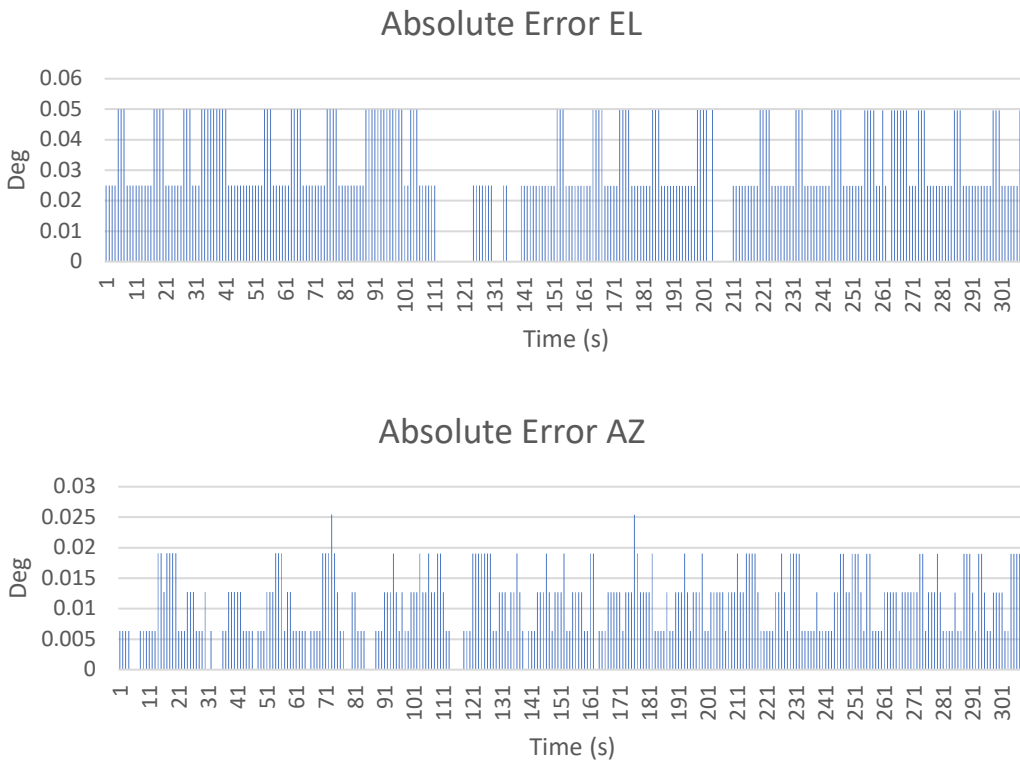


**Figure 92.** Az and El tracking error calculation of new software.

### 7.3 Theoretical Sun Position Calculation Improvement

The old heliostat control software used a sun tracking position calculator that was both complex to understand and difficult to implement for more modern sun tracking algorithms. The team investigated five potential algorithms in the solar industry to replace the old calculator and down selected to a system developed by ENEA (Italy Solar Research Center). This algorithm shows a tolerance of  $0.0027^\circ$  accuracy that will stay within these bounds for 100 years [1]. The algorithm was originally written in CPP programming language, which was interpreted into the LabVIEW programming language by the NSTTF engineers to allow the necessary connectivity with the NSTTF Heliostat Control Software.

Figure 93 presents a tracking calculation taken on August 24<sup>th</sup>, 2023, with data points taken every hour. Figure 94 presents a percent error from the old software sun calculation against the new ENEA sun tracking calculation in both Azimuth and Altitude.

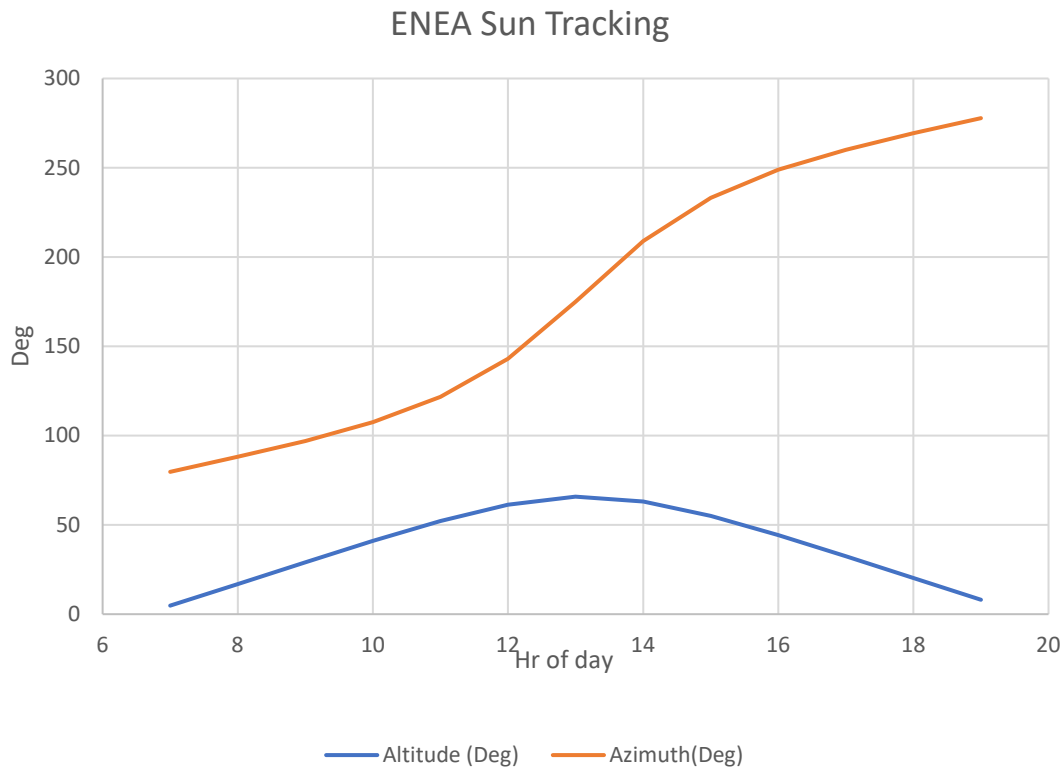


**Figure 93.** August 24<sup>th</sup>, 2023 ENEA Sun Tracking



**Figure 94.** Sun Tracking Error of Old Sun Tracking Calculator

## 8. REFERENCES

- [1] Grena, Roberto. "Five new algorithms for the computation of sun position from 2010 to 2110." *Solar Energy* 86.5 (2012): 1323-1337.
- [2] Strachan, John W. *Revisiting the BCS, a measurement system for characterizing the optics of solar collectors*. No. SAND-92-2789C; CONF-930561-6. Sandia National Labs., Albuquerque, NM (United States), 1992.

**DISTRIBUTION****Email—Internal**

<b>Name</b>	<b>Org.</b>	<b>Sandia Email Address</b>
Robert Keene	08925	<a href="mailto:rskeene@sandia.gov">rskeene@sandia.gov</a>
Kenneth Armijo	08925	<a href="mailto:kmarmij@sandia.gov">kmarmij@sandia.gov</a>
Margaret Gordon	08923	<a href="mailto:megord@sandia.gov">megord@sandia.gov</a>
Technical Library	01911	<a href="mailto:sanddocs@sandia.gov">sanddocs@sandia.gov</a>

**Email—External**

<b>Name</b>	<b>Institution</b>	<b>Sandia Email Address</b>
David Haas	U.S. DOE	<a href="mailto:David.Haas@ee.doe.gov">David.Haas@ee.doe.gov</a>



Sandia  
National  
Laboratories

Sandia National Laboratories is a multimission laboratory managed and operated by National Technology & Engineering Solutions of Sandia LLC, a wholly owned subsidiary of Honeywell International Inc. for the U.S. Department of Energy's National Nuclear Security Administration under contract DE-NA0003525.